Implementation of Mixed Finite Element Methods for Elliptic Equations on General Geometry

Todd Arbogast   Clint Dawson
Philip Keenan   Mary Wheeler
Ivan Yotov

CRPC-TR95525-S
March 1995

Center for Research on Parallel Computation
Rice University
6100 South Main Street
CRPC - MS 41
Houston, TX 77005

IMPLEMENTATION OF MIXED FINITE ELEMENT METHODS FOR ELLIPTIC EQUATIONS ON GENERAL GEOMETRY*

TODD ARBOGAST[†], CLINT N. DAWSON[†],
PHILIP T. KEENAN[†], MARY F. WHEELER[†], AND IVAN YOTOV[†]

Abstract. We consider the efficient implementation of mixed finite elements for solving second order elliptic partial differential equations on geometrically general domains, concentrating on the lowest-order Raviart-Thomas approximating spaces. We consider the standard mixed method and its hybrid form, and the recently introduced expanded mixed method. The standard method yields a saddle-point linear system, and while the hybrid method yields a positive definite linear system, it has many more unknowns, one per element edge or face. The expanded mixed method is similar in its structure; however, we give a generalization of the method combined with a global mapping technique that makes it suitable for general meshes. Moreover, two quadrature rules are given which reduce the method to a cell-centered finite difference method on meshes of quadrilaterals or triangles in 2 dimensions and hexahedra or tetrahedra in 3 dimensions. This approach substantially reduces the complexity of the mixed finite element matrix, leaving a symmetric, positive definite system for only as many unknowns as elements. On smooth meshes that are either logically rectangular or triangular with six triangles per internal vertex, this finite difference method is as accurate as the standard mixed method; on non-smooth meshes it can lose accuracy. An enhancement of the method is defined that combines numerical quadrature with Lagrange multiplier pressures on certain element edges or faces. The enhanced method regains the accuracy of the solution on non-smooth meshes, with little additional cost if the mesh geometry is piece-wise smooth, as in hierarchical meshes. Theoretical error estimates and numerical examples are given comparing the accuracy and efficiency of the methods.

Key words. mixed finite element, finite difference, elliptic partial differential equation, tensor coefficient, error estimates, logically rectangular grids, irregular meshes, unstructured meshes

AMS(MOS) subject classifications. 65N06, 65N12, 65N15, 65N22, 65N30

1. Introduction. We discuss several variations of the mixed finite element method [31, 9] for solving a second order elliptic problem posed on a possibly irregular domain $\Omega \subseteq \mathbf{R}^d$, $d = 2$ or 3. The problem is to find $(\mathbf{u}, p)$ such that

$$\mathbf{u} = -K \nabla p \qquad \text{in } \Omega, \tag{1.1a}$$

$$\alpha p + \nabla \cdot \mathbf{u} = f \quad \text{in } \Omega, \tag{1.1b}$$

$$p = g^D \qquad \text{on } \Gamma^D, \tag{1.1c}$$

$$\mathbf{u} \cdot \nu = g^N \qquad \text{on } \Gamma^N, \tag{1.1d}$$

where $\alpha \geq 0$, f, g^D, and g^N are smooth functions, K is a symmetric, positive definite second order tensor with smooth components, ν is the outward unit normal

† Department of Computational and Applied Mathematics, Mail Stop 134, Rice University, Houston, Texas 77251–1892.

vector on $\partial\Omega$, and $\partial\Omega$ is decomposed into Γ^D and Γ^N. For simplicity, assume that Γ^D is not empty or α is bounded away from zero, so that (1.1) has a unique solution. In applications to flow in porous media, p is the pressure, $\mathbf{u}$ is the velocity field, K is related to the permeability tensor, and α is related to the rock compressibility.

The mixed method is especially useful for problems where the velocity or strain $\mathbf{u} = -K\nabla p$ is an important quantity, since, in general, mixed methods approximate $\mathbf{u}$ to at least the order of accuracy of p. Furthermore, the approximate velocity calculated by the mixed method satisfies the conservation principle (1.1b) locally, not merely in a global sense as with standard Galerkin methods. This property is important in applications where local conservation of mass is desired.

Convergence and super-convergence properties of the mixed method are fairly well understood (see, e.g., [34, 31, 16, 27, 20, 36, 18, 19]), and many mixed finite element spaces satisfying the inf-sup or LBB condition [4, 5] are well known (e.g., [34, 31, 28, 8, 6, 7, 11]). Any geometrically general polygonal or polyhedral domain Ω can be partitioned into combinations of triangles and quadrilaterals in two dimensions and tetrahedra, prisms, and hexahedral elements in three. Most mixed spaces are defined only on standard, regular reference elements (an equilateral triangle or a square in two dimensions and a regular tetrahedron, a cube, or a regular equilateral prism in three dimensions); however, Thomas [34] described how to relate reference elements to the desired element shapes (triangles, quadrilaterals, tetrahedra, hexahedra, or prisms) through the use of affine or multi-linear maps and the Piola transformation (which preserves the normal component of vectors across boundaries).

Since the standard implementation of the mixed method yields a linear system that represents a saddle-point problem (as in §3.1 below), much current research involves how to efficiently solve such systems (see, e.g., [32, 22, 21, 33, 14, 29, 13, 2]). This is a particular problem when the domain is irregular.

The difficulty of the solution process can be eased by reformulating or further approximating the mixed method so that it yields a positive definite linear system. As Arnold and Brezzi [3] pointed out, this can be done directly by using the hybrid form of the mixed method: it is entirely equivalent to the mixed method. The introduction of additional Lagrange multiplier pressure unknowns allows one to eliminate the velocity and the original pressure unknowns from the system (as in §3.2 below). A positive definite system results, but at the expense of greatly increasing the number of unknowns. Our work is motivated by the desire to use the lowest order Raviart-Thomas mixed space RT_0 [31, 28], since these are widely used in practice and have the fewest number of unknowns. In this case, the hybrid form reduces to a face-centered finite difference method for the Lagrange pressures, one for each edge (if $d = 2$) or face (if $d = 3$).

In petroleum reservoir simulation, mixed finite element methods disguised as cell-centered finite difference methods have been the standard approach for many years [30]. The relationship between the mixed method and cell-centered finite differences on rectangular grids was first established in [32] under the assumption that K in (1.1) is a scalar or a diagonal matrix, and later in general in [2] for a variant of the mixed method, the "expanded mixed method" [37, 25, 10, 2]. The primary

restrictive assumption is that the mesh is rectangular. If one uses the RT_0 space and applies appropriate quadrature rules, the velocity unknowns can be eliminated and the method reduces to a positive definite, cell-centered finite difference method for the pressure p with a stencil of 9 points if $d = 2$ and 19 points if $d = 3$ (but only 5 or 7, respectively, if K is diagonal). This method achieves super-convergence (also called supra-convergence) at certain discrete points for both the pressure and velocity approximations [35, 26, 36, 2], and the number of unknowns is reduced to the number of cells or elements (which is much less than the number of edges or faces).

In this paper, we extend these cell-centered finite difference techniques to non-rectangular domains; that is, we will generalize the expanded mixed method, and then approximate it so that it gives a cell-centered finite difference method on irregular meshes, including logically rectangular and triangular meshes. We also assess the accuracy of the mehod, and compare it to and improve it with the hybrid formulation.

Thomas' approach [34] was to partition Ω locally into elements with straight edges and then to map each to a reference element by an affine or a multi-linear mapping. As we will see, in order to maintain accuracy, we need to consider a global approach. We assume that there is some reference or computational domain $\hat{\Omega}$ that has been partitioned into standard affine elements. (Affine elements are the image by an affine map of a standard, regular reference element; this does not include quadrilaterals or hexahedra.) Further, a single global map takes $\hat{\Omega}$ to the true domain Ω. This then defines curved element domains on Ω. (This mapping idea is not new, of course; our work was partly motivated by [1], where a global C^2 map is generated for mapping a rectangular computational domain to a simply connected true domain.)

The mixed finite element spaces are defined in the standard way on the reference partition and by Piola transformation on the curved elements. After mapping the original problem on Ω to $\hat{\Omega}$, all further computations can be performed on the reference, computational domain if desired. The mapped problem is of the same form as (1.1) in which Ω is replaced by $\hat{\Omega}$ and the data are modified in a simple way (though K is transformed as a tensor); that is, (1.1) on the general domain Ω is reduced to a similar problem on the (presumably) simpler computational domain $\hat{\Omega}$. This is especially advantageous in time dependent problems such as appear in flow in porous media in which $K(x,t) = K_1(x,t)K_2(x)$ and K_1 is a scalar, since the tensor K_2 need be transformed only once at the beginning of the calculation.

If the computational domain has a rectangular grid, the induced grid is logically rectangular, and the data structures of a computer code may reflect this, simplifying its structure. Moreover, we will show that super-convergence is obtained by the discrete solution, provided that the true mesh is reasonably smooth.

We also derive a quadrature rule for triangular elements which reduces the expanded mixed method to a cell-centered finite difference method for the pressure. In two dimensions, the finite difference stencil has ten points. We demonstrate by computational example and mathematical proof that the method is easy to solve

and is as accurate as the mixed method, provided again that the triangulation is smooth.

If the true mesh is not smooth (in a sense to be defined), there can be an undesirable loss of accuracy in the solution. This loss is caused by discontinuities in the mapping function (and is inevitable for tetrahedral meshes). Nevertheless, our ideas are useful for non-smooth meshes for two reasons. First, the method can be used as a preconditioner for the mixed method without quadrature, and, second, the loss of accuracy can be avoided by enhancing the method with Lagrange multiplier pressures on element faces where the discontinuities appear.

The rest of this paper is outlined as follows. In the next section we give some notation used throughout the paper. We review briefly the standard and hybrid mixed methods and present our generalization of the expanded mixed method in §3, emphasizing aspects of the solution process. In §4 we recall the construction of mixed elements on general shaped domains; that is, certain properties of change of variables and Piola transformation, as well as the construction of the mixed finite element spaces on quadrilaterals and hexahedra. Furthermore, our generalization of the usual mixed spaces on affine elements to curved elements is given in this section. Our application to general geometry domains is discussed in §5, and we restrict attention to logically rectangular grids and triangular elements in §§6–7. Convergence results are given in §8, and computational results that demonstrate these results and the relative efficiencies of the various methods are presented in §9. The enhanced finite difference method is given in §10, a remark about discontinuities in the standard mixed method is made in §11, and finally some conclusions are given in the last section.

2. Some general notation. Let $L^q(R)$ denote the standard Sobolev space of q-integrable functions on a domain $R \subset \mathbf{R}^d$. We denote by $(\,\cdot\,,\,\cdot\,)_R$ the $L^2(R)$ inner product or duality pairing, and the $L^2(R)$ norm is denoted by

$$\|\psi\|_{0,R} = (\psi, \psi)_R^{1/2}.$$

Let $\langle\cdot,\cdot\rangle_{\partial R}$ be the $L^2(\partial R)$ inner product or duality pairing. Define

$$H(\text{div}; R) = \{\mathbf{v} \in (L^2(R))^d : \nabla \cdot \mathbf{v} \in L^2(R)\},$$

with the norm

$$\|\mathbf{v}\|_{H(\text{div};R)} = \left\{ \int_R \left(|\mathbf{v}|^2 + |\nabla \cdot \mathbf{v}|^2\right) dx \right\}^{1/2}.$$

Furthermore, let $W^{j,q}(R)$ be the Sobolev space of j-times differentiable functions in $L^q(R)$. Let simply $H^j(R) = W^{j,2}(R)$, and $H^{-j}(R) = (H^j(R))'$ be its dual space. Let $\|\cdot\|_{j,q,R}$ denote the norm of $W^{j,q}(R)$, $\|\cdot\|_{j,R}$ denote the norm of $H^j(R)$, and $\|\cdot\|_{-j,R}$ denote the norm of its dual space $H^{-j}(R)$. When $R = \Omega$, we may omit it in the definitions above.

Let $\{\mathcal{E}_h\}_{h>0}$ be a regular family of finite element partitions of Ω [12], where h is the maximal element diameter, such that each element edge or face on the domain boundary is contained entirely within either Γ^D or Γ^N. Suppressing h, let

N_E denote the number of elements in $\mathcal{E}_h$, N_e the number of edges or faces, and N_e^N and N_e^D the number of edges or faces in Γ^N and Γ^D, respectively. Generally speaking, $N_e^N \ll N_e$.

Associate with $\mathcal{E}_h$ the mixed finite element space $V_h \times W_h \subset H(\mathrm{div}; \Omega) \times L^2(\Omega)$, for example, the RT or RTN spaces [34, 31, 28], BDM spaces [8], BDFM spaces [7], BDDF spaces [6], or CD spaces [11]. Let Λ_h denote the full space of Lagrange multipliers associated with $V_h \times W_h$; these functions are defined in a piecewise discontinuous manner on the edges or faces of the elements e as $V_h|_e \cdot \nu$. Let Λ_h^N denote the space of Lagrange multipliers restricted to Γ^N. Finally, let $\bar{V}_h$ denote the piecewise discontinuous version of V_h; that is, the space such that $\bar{V}_h|_E = V_h|_E$ for all elements $E \in \mathcal{E}_h$, but with no constraint that the space be in $H(\mathrm{div}; \Omega)$. Let N_V, $N_{\bar{V}}$, N_W, N_Λ, and N_{Λ^N} denote the dimensions of V_h, $\bar{V}_h$, W_h, Λ_h, and Λ_h^N, respectively, and let us choose some standard bases:

$$V_h = \mathrm{span}\{\mathbf{v}_j,\ j = 1, \dots, N_V\},$$
$$\bar{V}_h = \mathrm{span}\{\bar{\mathbf{v}}_j,\ j = 1, \dots, N_{\bar{V}}\},$$
$$W_h = \mathrm{span}\{w_i,\ i = 1, \dots, N_W\},$$
$$\Lambda_h = \mathrm{span}\{\mu_k,\ k = 1, \dots, N_\Lambda\},$$
$$\Lambda_h^N = \mathrm{span}\{\mu_k,\ k = 1, \dots, N_{\Lambda^N}\}.$$

We describe the approximation properties of these spaces by l_V and l_W such that

$$(2.1) \qquad \min_{\mathbf{v} \in V_h} \|\mathbf{q} - \mathbf{v}\|_0 \le C\|\mathbf{q}\|_l\, h^l, \qquad 1 \le l \le l_V,$$

$$(2.2) \qquad \min_{w \in W_h} \|\psi - w\|_0 \le C\|\psi\|_l\, h^l, \qquad 0 \le l \le l_W,$$

$$(2.3) \qquad \min_{\mathbf{v} \in V_h} \|\nabla \cdot (\mathbf{q} - \mathbf{v})\|_0 \le C\|\nabla \cdot \mathbf{q}\|_l\, h^l, \quad 0 \le l \le l_W.$$

For the RTN and BDFM spaces, $l_W = l_V$, while for the BDM and BDDF spaces, $l_W = l_V - 1$. The CD spaces are a generalization of these spaces on prisms.

For later reference, we recall the definition of the RT_0 space in its standard nodal basis. For all elements,

$$W_h = \mathrm{span}\{w_i,\ i = 1, \dots, N_E : w_i|_{E_\ell} = \delta_{i\ell},\ \ell = 1, \dots, N_E\}$$

and

$$\Lambda_h = \mathrm{span}\{\mu_k,\ k = 1, \dots, N_e : \mu_k|_{e_\ell} = \delta_{k\ell},\ \ell = 1, \dots, N_e\}$$

(i.e., each is a set of piecewise discontinuous constant functions). Let ν_j denote one of the unit vectors normal to edge or face e_j. If $d = 3$ and $E \in \mathcal{E}_h$ is a tetrahedron, let

$$V_h(E) = \big\{\mathbf{v} = (v^1, v^2, v^3) :$$
$$v^\ell|_E = a^\ell + bx_\ell,\ \ell = 1, 2, 3,\ \text{for some 4 constants } a^\ell \text{ and } b\big\},$$

and if $E \in \mathcal{E}_h$ is a rectangular parallelepiped, let

$$V_h(E) = \big\{ \mathbf{v} = (v^1, v^2, v^3) :$$
$$v^\ell|_E = a^\ell + b^\ell x_\ell, \ \ell = 1, 2, 3, \text{ for some 6 constants } a^\ell \text{ and } b^\ell \big\},$$

with a similar definition if $d = 2$. Then

$$(2.4) \quad V_h = \text{span}\big\{ \mathbf{v}_j \in H(\text{div}; \Omega), \ j = 1, \ldots, N_e :$$
$$\mathbf{v}_j|_E \in V_h(E) \text{ for all } E \in \mathcal{E}_h \text{ and } \mathbf{v}_j \cdot \nu_\ell|_{e_\ell} = \delta_{j\ell}, \ \ell = 1, \ldots, N_e \big\};$$

thus, $\mathbf{v}_j$ is nonzero only on the two elements which share edge j, and the normal component of the vectors match across e_j. Finally $\bar{V}_h$ has no matching condition, so $N_{\bar{V}} = 2N_e - N_e^N - N_e^D$. For RT_0, $l_V = l_W = 1$.

Let $(\cdot, \cdot)_{R,\mathbf{M}}$ denote an application of the midpoint quadrature rule to the $L^2(R)$ inner product on R with respect to $\mathcal{E}_h$. If the mesh is rectangular, let $(\cdot, \cdot)_{R,\mathbf{T}}$ denote an application of the trapezoidal rule. For RT_0 on rectangular grids, we will also need to refer to the trapezoidal-midpoint rule, defined for vectors $\mathbf{v} = (v_1, v_2, v_3)$ and $\mathbf{q} = (q_1, q_2, q_3)$ as

$$(\mathbf{v}, \mathbf{q})_{R,\mathbf{TM}} = (v_1, q_1)_{R,\mathbf{T}\times\mathbf{M}\times\mathbf{M}} + (v_2, q_2)_{R,\mathbf{M}\times\mathbf{T}\times\mathbf{M}} + (v_3, q_3)_{R,\mathbf{M}\times\mathbf{M}\times\mathbf{T}};$$

that is, for $i = 1, 2, 3$, the ith integral on the right side uses the trapezoidal rule in x_i and the midpoint rule in the other coordinate directions. If $\mathbf{v}, \mathbf{q} \in V_h$ (RT_0), then $\mathbf{TM}$ uses exactly the nodal points, and the trapezoidal and $\mathbf{TM}$ rules are equivalent. For any of our quadrature rules, let

$$\|\psi\|_{R,\mathbf{Q}} = (\psi, \psi)^{1/2}_{R,\mathbf{Q}}.$$

Again, we may omit R if it is Ω.

3. The standard, hybrid, and expanded mixed methods. We first review the standard and hybrid mixed methods, and then present our version of an expanded method.

3.1 The standard mixed method. A mixed variational form of (1.1) is

$$(3.1.1a) \qquad (K^{-1}\mathbf{u}, \mathbf{v}) - (p, \nabla \cdot \mathbf{v})$$
$$= -\langle g^D, \mathbf{v} \cdot \nu \rangle_{\Gamma^D} - \langle p, \mathbf{v} \cdot \nu \rangle_{\Gamma^N}, \quad \mathbf{v} \in H(\text{div}; \Omega),$$

$$(3.1.1b) \qquad (\alpha p, w) + (\nabla \cdot \mathbf{u}, w) = (f, w), \qquad w \in L^2(\Omega),$$

$$(3.1.1c) \qquad \langle \mathbf{u} \cdot \nu, \mu \rangle_{\Gamma^N} = \langle g^N, \mu \rangle_{\Gamma^N}, \qquad \mu \in H^{1/2}(\Gamma^N).$$

In the standard mixed method, we seek $\mathbf{U} \in V_h$, $P \in W_h$, and $\lambda \in \Lambda_h^N$ satisfying

$$(3.1.2a) \qquad (K^{-1}\mathbf{U}, \mathbf{v}) - (P, \nabla \cdot \mathbf{v})$$
$$= -\langle g^D, \mathbf{v} \cdot \nu \rangle_{\Gamma^D} - \langle \lambda, \mathbf{v} \cdot \nu \rangle_{\Gamma^N}, \quad \mathbf{v} \in V_h,$$

$$(3.1.2b) \qquad (\alpha P, w) + (\nabla \cdot \mathbf{U}, w) = (f, w), \qquad w \in W_h,$$

$$(3.1.2c) \qquad \langle \mathbf{U} \cdot \nu, \mu \rangle_{\Gamma^N} = \langle g^N, \mu \rangle_{\Gamma^N}, \qquad \mu \in \Lambda_h^N.$$

Here we have imposed the Neumann boundary condition weakly; however, it can also be imposed strongly, in which case λ is unnecessary.

Let

$$\mathbf{U} = \sum_{i=1}^{N_V} \check{U}_i \mathbf{v}_i, \qquad P = \sum_{i=1}^{N_W} \check{P}_i w_i, \qquad \lambda = \sum_{i=1}^{N_\Lambda} \check{\lambda}_i \mu_i,$$

and define matrices

(3.1.3) $A_{j\ell} = (K^{-1}\mathbf{v}_j, \mathbf{v}_\ell), \quad j, \ell = 1, \dots, N_V,$

(3.1.4) $B_{ij} = (w_i, \nabla \cdot \mathbf{v}_j), \quad i = 1, \dots, N_W, \ j = 1, \dots, N_V,$

(3.1.5) $C_{jk} = \langle \mathbf{v}_j \cdot \nu, \mu_k \rangle_{\Gamma^N}, \quad j = 1, \dots, N_V, \ k = 1, \dots, N_{\Lambda^N},$

(3.1.6) $D_{i\ell} = (\alpha w_i, w_\ell), \quad i, \ell = 1, \dots, N_W.$

Then (3.1.2) yields a system of the form

(3.1.7)
$$\begin{pmatrix} -A & B^T & -C \\ B & D & 0 \\ -C^T & 0 & 0 \end{pmatrix} \begin{pmatrix} \check{U} \\ \check{P} \\ \check{\lambda} \end{pmatrix} = \begin{pmatrix} \check{g}^D \\ \check{f} \\ -\check{g}^N \end{pmatrix},$$

which is indefinite. The Shur complement system for the pressure unknowns is easily extracted as
(3.1.8)
$$\left\{ \begin{pmatrix} B \\ -C^T \end{pmatrix} A^{-1} \begin{pmatrix} B^T & -C \end{pmatrix} + \begin{pmatrix} D & 0 \\ 0 & 0 \end{pmatrix} \right\} \begin{pmatrix} \check{P} \\ \check{\lambda} \end{pmatrix} = \begin{pmatrix} \check{f} \\ -\check{g}^N \end{pmatrix} + \begin{pmatrix} B \\ -C^T \end{pmatrix} A^{-1} \check{g}^D,$$

which is positive definite, but in general full because of the presence of A^{-1}. When using an iterative method such as conjugate gradient iteration to solve this system, applying the matrix inside the curly braces to a vector involves solving a second system of equations involving the matrix A, which can be inefficient, even for RT_0.

3.2 The hybrid form of the mixed method. The hybrid mixed method is based on the variational form (3.1.1). We seek $\mathbf{U} \in \bar{V}_h$, $P \in W_h$, and $\lambda \in \Lambda_h$ satisfying

(3.2.1a) $(K^{-1}\mathbf{U}, \mathbf{v}) = \sum_{E \in \mathcal{E}_h} \big[(P, \nabla \cdot \mathbf{v})_E - \langle g^D, \mathbf{v} \cdot \nu \rangle_{\partial E \cap \Gamma^D}$

$$- \langle \lambda, \mathbf{v} \cdot \nu \rangle_{\partial E \setminus \Gamma^D} \big], \qquad \mathbf{v} \in \bar{V}_h,$$

(3.2.1b) $(\alpha P, w) + \sum_{E \in \mathcal{E}_h} (\nabla \cdot \mathbf{U}, w)_E = (f, w), \qquad w \in W_h,$

(3.2.1c) $\sum_{E \in \mathcal{E}_h} \langle \mathbf{U} \cdot \nu, \mu \rangle_{\partial E} = \sum_{E \in \mathcal{E}_h} \langle g^N, \mu \rangle_{\partial E \cap \Gamma^N}, \qquad \mu \in \Lambda_h.$

Since (3.2.1c) forces $\mathbf{U} \cdot \nu$ to agree on both sides of any edge or face, in fact $\mathbf{U} \in V_h$ and the standard and hybrid methods are equivalent [3].

Define matrices A, B, C, and D analogous to (3.1.3)–(3.1.6) above for $\bar{V}_h$, $N_{\bar{V}}$, Λ_h, and N_Λ replacing V_h, N_V, Λ_h^N, and N_{Λ^N}, respectively. Then (3.2.1) yields a

system of the form (3.1.8). Now, however, A is element-wise block diagonal, since $\bar{V}_h$ has no continuity constraints. Its inverse is easily found and a sparse matrix results [3]. Furthermore, $BA^{-1}B^T + D$ is diagonal, so we can also eliminate $\check{P}$ to obtain

$$
\begin{aligned}
(3.2.2) \quad &\{C^T A^{-1} C - C^T A^{-1} B^T (BA^{-1}B^T + D)^{-1} BA^{-1}C\}\check{\lambda} \\
&= -\check{g}^N - C^T A^{-1}\check{g}^D + C^T A^{-1} B^T (BA^{-1}B^T + D)^{-1}\left[BA^{-1}\check{g}^D + \check{f}\right].
\end{aligned}
$$

This is a sparse, positive definite system; however, since the Lagrange pressures live on the element edges or faces, it is a face-centered finite difference method.

For RT_0, there is one unknown per edge or face, which is anywhere from 1.5 to 3 times as many as the number of cells, depending on the spatial dimension and whether simplicial or rectangular elements are used.

3.3 The expanded mixed method. A second, expanded mixed variational form of (1.1) can be given as follows. Let G be some symmetric, positive definite tensor function, to be defined later in terms of the local geometry, and expand the system (1.1) by introducing the "adjusted gradient"

$$
(3.3.1) \qquad\qquad\qquad \tilde{\mathbf{u}} = -G\nabla p.
$$

Then

$$
(3.3.2) \qquad\qquad\qquad \mathbf{u} = KG^{-1}\tilde{\mathbf{u}}
$$

and

$$
(3.3.3\text{a}) \qquad (G^{-1}\mathbf{u}, \tilde{\mathbf{v}}) = (G^{-1}KG^{-1}\tilde{\mathbf{u}}, \tilde{\mathbf{v}}), \qquad \tilde{\mathbf{v}} \in (L^2(\Omega))^d,
$$

$$
\begin{aligned}
(3.3.3\text{b}) \qquad &(G^{-1}\tilde{\mathbf{u}}, \mathbf{v}) - (p, \nabla \cdot \mathbf{v}) \\
&= -\langle g^D, \mathbf{v}\cdot\nu\rangle_{\Gamma^D} - \langle p, \mathbf{v}\cdot\nu\rangle_{\Gamma^N}, \quad \mathbf{v} \in H(\mathrm{div}; \Omega),
\end{aligned}
$$

$$
(3.3.3\text{c}) \qquad (\alpha p, w) + (\nabla\cdot\mathbf{u}, w) = (f, w), \qquad w \in L^2(\Omega),
$$

$$
(3.3.3\text{d}) \qquad \langle\mathbf{u}\cdot\nu, \mu\rangle_{\Gamma^N} = \langle g^N, \mu\rangle_{\Gamma^N}, \qquad\qquad \mu \in H^{1/2}(\Gamma^N).
$$

In the usual expanded formulation, G is taken to be the identity.

In the recently introduced expanded mixed method [37, 25, 10, 2], we need an additional finite element space $\tilde{V}_h$ such that $V_h \subseteq \tilde{V}_h \subseteq (L^2(\Omega))^d$. Let

$$
\tilde{V}_h = \mathrm{span}\{\tilde{\mathbf{v}}_m : m = 1,\dots,N_{\tilde{V}}\}.
$$

In our modification to the expanded mixed method, we seek $\mathbf{U} \in V_h$, $\tilde{\mathbf{U}} \in \tilde{V}_h$,

$P \in W_h$, and $\lambda \in \Lambda_h^N$ satisfying

(3.3.4a) $$(G^{-1}\mathbf{U}, \tilde{\mathbf{v}}) = (G^{-1}KG^{-1}\tilde{\mathbf{U}}, \tilde{\mathbf{v}}), \qquad \tilde{\mathbf{v}} \in \tilde{V}_h,$$

(3.3.4b) $$(G^{-1}\tilde{\mathbf{U}}, \mathbf{v}) - (P, \nabla \cdot \mathbf{v})$$
$$= -\langle g^D, \mathbf{v} \cdot \nu \rangle_{\Gamma^D} - \langle \lambda, \mathbf{v} \cdot \nu \rangle_{\Gamma^N}, \quad \mathbf{v} \in V_h,$$

(3.3.4c) $$(\alpha P, w) + (\nabla \cdot \mathbf{U}, w) = (f, w), \qquad w \in W_h,$$

(3.3.4d) $$\langle \mathbf{U} \cdot \nu, \mu \rangle_{\Gamma^N} = \langle g^N, \mu \rangle_{\Gamma^N}, \qquad \mu \in \Lambda_h^N.$$

This method is not equivalent to the standard method, except in trivial cases.

If we define

(3.3.5) $$A_{1,m\ell} = (G^{-1}KG^{-1}\tilde{\mathbf{v}}_m, \tilde{\mathbf{v}}_\ell), \quad m, \ell = 1, \ldots, N_{\tilde{V}},$$

(3.3.6) $$A_{2,jm} = (G^{-1}\mathbf{v}_j, \tilde{\mathbf{v}}_m), \qquad j = 1, \ldots, N_V, \ m = 1, \ldots, N_{\tilde{V}},$$

and B, C, and D as in (3.1.4)–(3.1.6), then (3.3.4) yields a system of the form

(3.3.7) $$\begin{pmatrix} A_1 & -A_2^T & 0 & 0 \\ -A_2 & 0 & B^T & -C \\ 0 & B & D & 0 \\ 0 & -C^T & 0 & 0 \end{pmatrix} \begin{pmatrix} \check{\tilde{U}} \\ \check{U} \\ \check{P} \\ \check{\lambda} \end{pmatrix} = \begin{pmatrix} 0 \\ \check{g}^D \\ \check{f} \\ -\check{g}^N \end{pmatrix},$$

which is indefinite. The Shur complement system for the pressure unknowns is now (3.1.8), wherein we replace

(3.3.8) $$A^{-1} = (A_2 A_1^{-1} A_2^T)^{-1}.$$

This is a positive definite system, but in general it is full.

This situation occurred for the standard mixed method. As mentioned in the introduction, in the special case of RT_0, rectangular elements, and a diagonal (or scalar) K, applying the trapezoidal-midpoint (**TM**) quadrature rule to (3.1.3) reduces A to a diagonal matrix [32]. The full matrix in (3.1.8) then becomes sparse with nonzero entries on five bands, and the cost of applying an iterative procedure to the solution of (3.1.8) is greatly reduced. In fact, the method reduces to the standard cell-centered finite difference method, with only as many unknowns as elements (up to some additional unknowns near Γ^N). Moreover, the accuracy of the approximate solutions is not compromised [36].

Recently, these ideas were exploited for (3.3.4) to obtain similar results [2]. Trapezoidal quadrature was applied to the integrals (3.3.5)–(3.3.6) defining A_1 and A_2, so that A_2 is diagonal when G is the identity. In the next four sections, we remove the restriction to rectangular meshes. We begin by considering carefully the finite element spaces on irregularly shaped elements.

4. The mixed finite element spaces for general elements. Many mixed finite element spaces are known, and the ones we considered can be constructed on a unit sized standard, regular reference element $\hat{E}$: an equilateral triangle, regular simplex, square, cube, or regular prism. An affine map then gives the definition on any triangle, tetrahedra, rectangular parallelepiped, or prism. The construction

of quadrilateral and hexahedral elements is more involved, and we review here the basic theory of Thomas [34]. We also generalize the mixed spaces, defined on $\hat{E}$, to curved elements.

4.1. Transformations for functions on $\hat{E}$. For any element E, let $F_E : \mathbf{R}^d \to \mathbf{R}^d$ be a smooth (at least C^1) mapping such that $F_E(\hat{E}) = E$, and let F_E be globally invertible on $\hat{E}$. Denote by $DF(\hat{\mathbf{x}})$ the Jacobian matrix of F_E ($DF_{ij} = \partial F_i / \partial x_j$), and let

$$J(\hat{\mathbf{x}}) = |\det(DF(\hat{\mathbf{x}}))|.$$

For any scalar function $\hat{\varphi}(\hat{\mathbf{x}})$ on $\hat{E}$, let

$$(4.1.1) \qquad \varphi(\mathbf{x}) = \mathcal{F}(\hat{\varphi})(\mathbf{x}) \equiv \hat{\varphi} \circ F_E^{-1}(\mathbf{x}).$$

LEMMA 4.1. *The operator $\mathcal{F}$ is an isomorphism of $L^2(\hat{E})$ onto $L^2(E)$ and of $H^1(\hat{E})$ onto $H^1(E)$.*

To construct a subspace of $H(\mathrm{div}; \Omega)$, we need to preserve the normal components of vector valued functions across the boundaries of the elements. We use the Piola transformation (see [34, 9]): For any function $\hat{\mathbf{q}} \in (L^2(\hat{E}))^d$, define

$$(4.1.2) \qquad \mathbf{q}(\mathbf{x}) = \mathcal{G}(\hat{\mathbf{q}})(\mathbf{x}) \equiv \left(\frac{1}{J} DF\, \hat{\mathbf{q}} \right) \circ F_E^{-1}(\mathbf{x}).$$

LEMMA 4.2. *The operator $\mathcal{G}$ is an isomorphism of $(L^2(\hat{E}))^d$ onto $(L^2(E))^d$ and of $H(\mathrm{div}; \hat{E})$ onto $H(\mathrm{div}; E)$. Moreover,*

$$(\mathbf{q}, \nabla\varphi)_E = (\hat{\mathbf{q}}, \hat{\nabla}\hat{\varphi})_{\hat{E}}, \quad \varphi \in H^1(E),\ \mathbf{q} \in (L^2(E))^d,$$

$$(\varphi, \nabla \cdot \mathbf{q})_E = (\hat{\varphi}, \hat{\nabla} \cdot \hat{\mathbf{q}})_{\hat{E}}, \quad \varphi \in L^2(E),\ \mathbf{q} \in H(\mathrm{div}; E).$$

4.2. Transformations for functions on $\partial\hat{E}$. For any function $\hat{\mu}(\hat{\mathbf{x}})$ defined on $\partial\hat{E}$, let

$$(4.2.1) \qquad \mu(\mathbf{x}) = \underline{\mathcal{F}}(\hat{\mu})(\mathbf{x}) \equiv \hat{\mu} \circ F_E^{-1}(\mathbf{x}).$$

LEMMA 4.3. *The operator $\underline{\mathcal{F}}$ is an isomorphism of $L^2(\partial\hat{E})$ onto $L^2(\partial E)$ and of $H^{1/2}(\partial\hat{E})$ onto $H^{1/2}(\partial E)$. Moreover, the trace of any function $\varphi \in H^1(E)$ on ∂E is the image by $\underline{\mathcal{F}}$ of the trace of $\hat{\varphi} = \mathcal{F}^{-1}(\varphi) \in H^1(\hat{E})$; that is,*

$$\hat{\varphi}|_{\partial\hat{E}} \overset{\underline{\mathcal{F}}}{\longleftrightarrow} \varphi|_{\partial E}.$$

Thus $\underline{\mathcal{F}}$ can be considered as the trace of $\mathcal{F}$ on ∂E. To define the trace of $\mathcal{G}$ on ∂E, for any function $\hat{\mu}^*$ on $\partial\hat{E}$, define

$$(4.2.2) \qquad \mu^*(\mathbf{x}) = \underline{\mathcal{G}}(\hat{\mu}^*)(\mathbf{x}) \equiv \left(\frac{1}{J_{\hat{\nu}}} \hat{\mu}^* \right) \circ F_E^{-1}(\mathbf{x}),$$

where

$$J_{\hat{\nu}}(\hat{\mathbf{x}}) = J(\hat{\mathbf{x}})|(DF^{-1})^T \hat{\nu}|.$$

LEMMA 4.4. *The operator $\underline{\mathcal{G}}$ is an isomorphism of $L^2(\partial\hat{E})$ onto $L^2(\partial E)$ and can be extended to an isomorphism of $H^{-1/2}(\partial\hat{E})$ onto $H^{-1/2}(\partial E)$. The normal trace of any function $\mathbf{q} \in H(\mathrm{div}; E)$ is the image by $\underline{\mathcal{G}}$ of the normal trace of $\hat{\mathbf{q}} = \mathcal{G}^{-1}(\mathbf{q}) \in H(\mathrm{div}; \hat{E})$; that is,*

$$\hat{\mathbf{q}} \cdot \hat{\nu} \xleftrightarrow{\mathcal{G}} \mathbf{q} \cdot \nu.$$

Moreover, for $\mathbf{q} \in H(\mathrm{div}; E)$, $\mu \in H^{1/2}(\partial E)$,

$$(4.2.3) \qquad \langle \mu, \mathbf{q} \cdot \nu \rangle_{\partial E} = \langle \hat{\mu}, \hat{\mathbf{q}} \cdot \hat{\nu} \rangle_{\partial\hat{E}}.$$

REMARK. Equation (4.2.3) states that the normal trace of an $H(\mathrm{div}; \hat{E})$ function is preserved in $H^{-1/2}(\partial\hat{E})$ after transformation by $\mathcal{G}$.

4.3. Construction of the mixed spaces on Ω. Let $\hat{V}_h(\hat{E}) \times \hat{W}_h(\hat{E})$ be any of our previously cited mixed spaces defined on the reference element $\hat{E}$. If $\mathcal{E}_h$ is a partition of Ω into elements of standard shape, Thomas [34] defined for Raviart-Thomas elements (and by extension, for the other families of elements) for each $E \in \mathcal{E}_h$

$$(4.3.1) \qquad V_h(E) = \{\mathbf{v} \in H(\mathrm{div}; E) : \mathbf{v} \xleftrightarrow{\mathcal{G}} \hat{\mathbf{v}} \in \hat{V}_h(\hat{E})\},$$

$$(4.3.2) \qquad W_h(E) = \{w \in L^2(E) : w \xleftrightarrow{\mathcal{F}} \hat{w} \in \hat{W}_h(\hat{E})\},$$

and then

$$(4.3.3) \qquad V_h(\Omega) = \{\mathbf{v} \in H(\mathrm{div}; \Omega) : \mathbf{v}|_E \in V_h(E), \ \forall E \in \mathcal{E}_h\},$$

$$(4.3.4) \qquad W_h(\Omega) = \{w \in L^2(\Omega) : w|_E \in W_h(E), \ \forall E \in \mathcal{E}_h\}.$$

REMARK. In the case of simplex or parallelogram elements, the map F_E is affine for any element E. When the elements are general quadrilaterals or hexahedra, F_E is non-affine, and some difficulties arise in the analysis and some loss in approximability occurs, either in rate or in the regularity needed [34].

We generalize the mixed spaces to curved elements in a straightforward way. Let $\hat{\Omega}$ be our computational reference domain and let

$$F : \mathbf{R}^d \to \mathbf{R}^d, \quad F(\hat{\Omega}) = \Omega,$$

be a smooth (at least C^2) invertible map. Let $\hat{\mathcal{E}}_{\hat{h}}$ be a regular family of partitions of $\hat{\Omega}$ into standard shaped elements. This gives a mesh on $\hat{\Omega}$, and its image by F is a curved mesh $\mathcal{E}_h$ on Ω. Let $\hat{V}_h \times \hat{W}_h$ be any of the usual mixed spaces defined over $\hat{\mathcal{E}}_{\hat{h}}$. The mixed spaces on $\mathcal{E}_h$ are defined by (4.3.1)–(4.3.4).

5. Application to general geometry. We use F to map the problem (1.1) and its mixed approximation on Ω to $\hat{\Omega}$ using the isomorphisms $\mathcal{F}$ and $\mathcal{G}$, defined in §4, for mapping scalar and vector functions, respectively.

Since for $\mathbf{u}, \mathbf{v} \in V_h$,

$$(5.1) \qquad K^{-1}\mathbf{u} \cdot \mathbf{v} = K^{-1}\left(\frac{1}{J}DF\,\hat{\mathbf{u}}\right) \cdot \left(\frac{1}{J}DF\,\hat{\mathbf{v}}\right) = \left(\frac{1}{J^2}\,DF^T K^{-1} DF\right)\hat{\mathbf{u}} \cdot \hat{\mathbf{v}},$$

the standard mixed method can be transformed easily. We seek $\hat{\mathbf{U}} \in \hat{V}_h$, $\hat{P} \in \hat{W}_h$, and $\hat{\lambda} \in \hat{\Lambda}_h^N$ satisfying

(5.2a)
$$\left(\frac{1}{J} DF^T K^{-1} DF \hat{\mathbf{U}}, \hat{\mathbf{v}} \right) - (\hat{P}, \hat{\nabla} \cdot \hat{\mathbf{v}})$$
$$= -\langle \hat{g}^D, \hat{\mathbf{v}} \cdot \hat{\nu} \rangle_{\hat{\Gamma}^D} - \langle \hat{\lambda}, \hat{\mathbf{v}} \cdot \hat{\nu} \rangle_{\hat{\Gamma}^N}, \quad \hat{\mathbf{v}} \in \hat{V}_h,$$

(5.2b)
$$(J \hat{\alpha} \hat{P}, \hat{w}) + (\hat{\nabla} \cdot \hat{\mathbf{U}}, \hat{w}) = (J \hat{f}, \hat{w}), \quad \hat{w} \in \hat{W}_h,$$

(5.2c)
$$\langle \hat{\mathbf{U}} \cdot \hat{\nu}, \hat{\mu} \rangle_{\hat{\Gamma}^N} = \langle J_{\hat{\nu}} \hat{g}^N, \hat{\mu} \rangle_{\hat{\Gamma}^N}, \quad \hat{\mu} \in \hat{\Lambda}_h^N.$$

The tensor K^{-1} has been modified in the standard method to

(5.3)
$$\mathcal{K}^{-1} = \frac{1}{J} DF^T K^{-1} DF.$$

For the expanded method, we make a careful choice of G in (3.3.1) to simplify the interaction of the basis functions in (3.3.6) on the computational domain $\hat{\Omega}$. Define

(5.4)
$$G(F(\hat{\mathbf{x}})) = \left(\frac{1}{J} DF \, DF^T \right) (\hat{\mathbf{x}}).$$

Note that G is symmetric and positive definite. It is easy to see that G is bounded for any of the spaces under consideration. Then,

(5.5)
$$G^{-1} \tilde{\mathbf{v}} \cdot \mathbf{v} = J (DF^{-1})^T DF^{-1} \left(\frac{1}{J} DF \, \hat{\tilde{\mathbf{v}}} \right) \cdot \left(\frac{1}{J} DF \, \hat{\mathbf{v}} \right) = \frac{1}{J} \hat{\tilde{\mathbf{v}}} \cdot \hat{\mathbf{v}}, \quad \mathbf{v}, \tilde{\mathbf{v}} \in \tilde{V}_h.$$

We obtain the following problem on the reference domain: Find $\hat{\mathbf{U}} \in \hat{V}_h$, $\hat{\tilde{\mathbf{U}}} \in \hat{\tilde{V}}_h$, $\hat{P} \in \hat{W}_h$, and $\hat{\lambda} \in \hat{\Lambda}_h^N$ such that

(5.6a)
$$(\hat{\mathbf{U}}, \hat{\tilde{\mathbf{v}}})_{\hat{\Omega}} = \left(J DF^{-1} K (DF^{-1})^T \hat{\tilde{\mathbf{U}}}, \hat{\tilde{\mathbf{v}}} \right)_{\hat{\Omega}}, \quad \hat{\tilde{\mathbf{v}}} \in \hat{\tilde{V}}_h,$$

(5.6b)
$$(\hat{\tilde{\mathbf{U}}}, \hat{\mathbf{v}})_{\hat{\Omega}} - (\hat{P}, \hat{\nabla} \cdot \hat{\mathbf{v}})_{\hat{\Omega}}$$
$$= -\langle \hat{g}^D, \hat{\mathbf{v}} \cdot \hat{\nu} \rangle_{\hat{\Gamma}^D} - \langle \hat{\lambda}, \hat{\mathbf{v}} \cdot \hat{\nu} \rangle_{\hat{\Gamma}^N}, \quad \hat{\mathbf{v}} \in \hat{V}_h,$$

(5.6c)
$$(J \hat{\alpha} \hat{P}, \hat{w})_{\hat{\Omega}} + (\hat{\nabla} \cdot \hat{\mathbf{U}}, \hat{w})_{\hat{\Omega}} = (J \hat{f}, \hat{w})_{\hat{\Omega}}, \quad \hat{w} \in \hat{W}_h,$$

(5.6d)
$$\langle \hat{\mathbf{U}} \cdot \hat{\nu}, \hat{\mu} \rangle_{\hat{\Gamma}^N} = \langle J_{\hat{\nu}} \hat{g}^N, \hat{\mu} \rangle_{\hat{\Gamma}^N}, \quad \hat{\mu} \in \hat{\Lambda}_h^N.$$

Note that $\hat{V}_h \times \hat{W}_h \times \hat{\Lambda}_h^N$ are the usual mixed spaces on reference elements, and $\hat{\tilde{V}}_h = \mathcal{F}^{-1}(\tilde{V}_h)$. Also, there are no coefficients in the L^2-vector inner-products on the left side of the first two equations. The tensor K has been modified in the expanded method to

(5.7)
$$\mathcal{K} = J DF^{-1} K (DF^{-1})^T,$$

which is equivalent to (5.3).

6. Cell-centered finite differences on logically rectangular grids. In this section we consider the RT_0 spaces on curved but logically rectangular grids. These are grids generated by taking a rectangular computational domain $\hat{\Omega}$, imposing on it a rectangular grid, and mapping it to Ω by the function F. It is not known how to approximate the standard mixed method (5.2) on rectangles so that a finite difference stencil results (i.e., the Shur complement system (3.1.8) is sparse), unless K is a diagonal tensor. For geometrically irregular domains, the transformed coefficient is necessarily a full tensor except in trivial cases. However, because of our choice (5.4) of G, the expanded problem on the computational grid (5.6) is the same as that analyzed in [2]. There, a finite difference stencil is derived for the pressure, when trapezoidal quadrature rules are used for evaluating three of the integrals. We exploit this result on general geometry.

Take $\tilde{V}_h = V_h$, so that A_2 of (3.3.6) is square and invertible. The scheme proposed in [2] approximating (5.6) on the computational domain is (5.6c)–(5.6d) combined with

$$(6.1a) \qquad (\hat{\mathbf{U}}, \hat{\tilde{\mathbf{v}}})_{\hat{\Omega},\mathbf{TM}} = (JDF^{-1}K(DF^{-1})^T\hat{\tilde{\mathbf{U}}}, \hat{\tilde{\mathbf{v}}})_{\hat{\Omega},\mathbf{T}}, \quad \hat{\tilde{\mathbf{v}}} \in \hat{\tilde{V}}_h,$$

$$(6.1b) \qquad (\hat{\tilde{\mathbf{U}}}, \hat{\mathbf{v}})_{\hat{\Omega},\mathbf{TM}} - (\hat{P}, \hat{\nabla} \cdot \hat{\mathbf{v}})_{\hat{\Omega}}$$

$$= -\langle \hat{g}^D, \hat{\mathbf{v}} \cdot \hat{\nu} \rangle_{\hat{\Gamma}^D} - \langle \hat{\lambda}, \hat{\mathbf{v}} \cdot \hat{\nu} \rangle_{\hat{\Gamma}^N}, \qquad \hat{\mathbf{v}} \in \hat{V}_h.$$

By the definition of RT_0, the trapezoidal or **TM** quadrature rule diagonalizes A_2 in (3.3.6) on the computational domain; that is, recalling that $\hat{V}_h = \text{span}\{\hat{\mathbf{v}}_j\}$ where $\{\hat{\mathbf{v}}_j\}$ is the nodal basis (2.4),

$$(6.2) \qquad \hat{A}_{2,jm} = (\hat{\mathbf{v}}_j, \hat{\mathbf{v}}_m)_{\hat{\Omega},\mathbf{TM}} = \hat{C}_h \delta_{jm}, \quad j, m = 1, \ldots N_e,$$

where $\hat{C}_h$ is a constant related to the mesh size. Since the two integrals in (6.1) involving **TM** quadrature are diagonal, the method gives a 19 point stencil if $d = 3$ and a 9 point stencil if $d = 2$ for $\hat{P}$ in the Shur complement form of (3.3.7), i.e., (3.1.8) and (3.3.8). This is an approximation to the expanded mixed method.

The approximation of our problem (1.1) is now relatively simple. A preprocessing step can be done to transform the coefficients (by multiplication by either J or $J_{\hat{\nu}}$, or by the tensor transformation (5.7)). Then (5.6a)–(5.6b), (6.1) is solved as an entirely rectangular problem. Finally, (4.1.1)–(4.1.2) (i.e., $\mathcal{F}$ and $\mathcal{G}$) map the results $\hat{P}$ and $\hat{\mathbf{U}}$ back to P and $\mathbf{U}$ on the physical domain as approximations to p and $\mathbf{u}$.

7. Cell-centered finite differences on triangles. In this section we consider $d = 2$ and a triangular mesh. Actually, on $\hat{\Omega}$, take a grid $\hat{\mathcal{E}}_h$ of equilateral triangles. As in the logically rectangular case, we need a quadrature rule for the triangular RT_0 mixed method that diagonalizes (6.2). Again, we take $\tilde{V}_h = V_h$.

Let $\hat{T}$ represent the standard reference equilateral triangle with vertices at $(-1, 0)$, $(1, 0)$, and $(0, \sqrt{3})$. Here let $\hat{\mathbf{v}}_k$ be the basis function of $\hat{V}_h(\hat{T})$ associated with edge k, denoted by $\hat{e}_k$, $k = 1, 2, 3$. We define our quadrature rule $\hat{Q}_{\hat{T}}(\psi)$ on $\hat{T}$

such that it is exact for polynomials of degree one, and $\hat{Q}_{\hat{T}}(\hat{\mathbf{v}}_k \cdot \hat{\mathbf{v}}_\ell) = 0$ for $k \neq \ell$:

$$(7.1) \qquad \hat{Q}_{\hat{T}}(\psi) = \frac{\sqrt{3}}{6}\left[\psi(-1,0) + \psi(1,0) + \psi(0,\sqrt{3}) + 3\psi\left(0,\frac{\sqrt{3}}{3}\right)\right].$$

The required properties follow easily from the definition of RT_0 given in §2. (Incidentally, this rule is second order accurate if the 6 is replaced by 12 and the 3 in front of the last term is replaced by 9, but then orthogonality is lost.) There is no corresponding rule on a non-equilateral triangle; it is necessary to consider the mapping to the reference element.

The scheme is now (5.6c)–(5.6d) combined with

$$(7.2a) \qquad \sum_{\hat{T}\in\hat{\mathcal{E}}_h} \hat{Q}_{\hat{T}}(\hat{\mathbf{U}} \cdot \hat{\tilde{\mathbf{v}}}) = (JDF^{-1}K(DF^{-1})^T\hat{\tilde{\mathbf{U}}}, \hat{\tilde{\mathbf{v}}})_{\hat{\Omega}}, \qquad\qquad \hat{\tilde{\mathbf{v}}} \in \hat{\tilde{V}}_h,$$

$$(7.2b) \qquad \sum_{\hat{T}\in\hat{\mathcal{E}}_h} \hat{Q}_{\hat{T}}(\hat{\tilde{\mathbf{U}}} \cdot \hat{\mathbf{v}}) - (\hat{P}, \hat{\nabla} \cdot \hat{\mathbf{v}})_{\hat{\Omega}} = -\langle \hat{g}^D, \hat{\mathbf{v}} \cdot \hat{\nu}\rangle_{\hat{\Gamma}^D} - \langle \hat{\lambda}, \hat{\mathbf{v}} \cdot \hat{\nu}\rangle_{\hat{\Gamma}^N}, \quad \hat{\mathbf{v}} \in \hat{V}_h.$$

Since the two integrals in (7.2) approximated by quadrature are diagonal, the method gives a 10 point stencil for $\hat{P}$ in the Shur complement form of (3.3.7), as shown in Fig. 7.1.
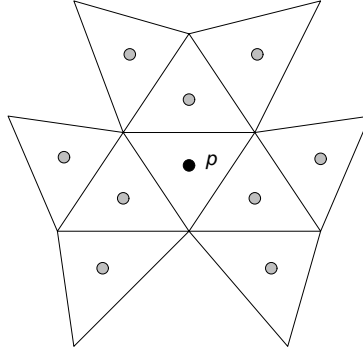

Fig. 7.1. Finite difference stencil for P.

The approximation of our problem (1.1) can be solved as in the logically rectangular case (transform coefficients, solve the transformed problem, and map the solution back to the physical domain). Since neither the physical mesh nor the computational mesh is orthogonal, in practice it may be simpler to compute this approximation to the expanded mixed method (3.3.3) directly on the physical mesh. In this case, we transform K by

$$(7.3) \qquad\qquad\qquad \mathcal{K} = G^{-1}KG^{-1},$$

and we approximate on each triangle $T \in \mathcal{E}_h$ in the integral evaluation routine

$$(7.4a) \qquad\qquad (G^{-1}\mathbf{u}, \tilde{\mathbf{v}})_T = (\hat{\mathbf{u}}, \hat{\tilde{\mathbf{v}}})_{\hat{T}} \approx \hat{Q}_{\hat{T}}(\hat{\mathbf{u}}, \hat{\tilde{\mathbf{v}}}),$$

$$(7.4b) \qquad\qquad (G^{-1}\tilde{\mathbf{u}}, \mathbf{v})_T = (\hat{\tilde{\mathbf{u}}}, \hat{\mathbf{v}})_{\hat{T}} \approx \hat{Q}_{\hat{T}}(\hat{\tilde{\mathbf{u}}}, \hat{\mathbf{v}}).$$

In three space dimensions, regular tetrahedra do not fill space, so there is no regular computational mesh. However, the approach described in this section can be extended in a local sense, using a similar quadrature rule on a regular tetrahedron. That is, take a tetrahedral mesh on Ω, such that each element $E \in \mathcal{E}_h$ is the image by F_E of a regular tetrahedron. Let $\hat{T}$ be the standard reference regular tetrahedron with vertices at $(-1, 0, 0)$, $(1, 0, 0)$, $(0, \sqrt{3}, 0)$ and $(0, \sqrt{3}/3, 2\sqrt{6}/3)$. Proceeding element-by-element, we diagonalize (6.2) by the first order approximation:

$$(7.5) \qquad \hat{Q}_{\hat{T}}(\psi) = \frac{\sqrt{2}}{18} \Big[\psi(-1, 0, 0) + \psi(1, 0, 0) + \psi(0, \sqrt{3}, 0)$$
$$+ \psi\left(0, \frac{\sqrt{3}}{3}, \frac{2\sqrt{6}}{3}\right) + 8\psi\left(0, \frac{\sqrt{3}}{3}, \frac{\sqrt{6}}{6}\right) \Big].$$

In this case, the stencil has at most seventeen nonzero entries. There is a problem with the accuracy of this method, and we will return to it in §10.

8. Some convergence results. With the notable exception of the work of Thomas [34], most of the known convergence estimates apply only to affine elements and special boundary elements. Recall that affine elements are the image by an affine map of an equilateral triangle, square, cube, regular simplex, or regular prism (i.e., the standard, regular reference elements), and that quadrilaterals and hexahedra are not affine elements. One feature of these affine and special boundary elements is that $\nabla \cdot V_h = W_h$. In this section we present some of these convergence results and extend them to curved elements, as defined at the end of §4.3.

Throughout this section, C will denote a generic positive constant that is independent of the discretization parameter h, may depend on Ω, and may depend on F only through $\|DF\|_{0,\infty}$ and $\|DF^{-1}\|_{0,\infty}$, unless other dependence is indicated explicitly. To quantify the dependence of the convergence on the mapping F, assuming $F \in (W^{\ell,\infty}(\hat{\Omega}))^{d \times d}$, we let $C_{F,\ell}$ be a generic constant that may depend on $\|F\|_{\ell,\infty}$ and $\|F^{-1}\|_{\ell,\infty}$.

To describe the super-convergence results for the pressure, denote the $L^2(\Omega)$-projection operator onto W_h by $\mathcal{P}_W$; that is, for $\psi \in L^2(\Omega)$, we define $\mathcal{P}_W\psi$ by

$$(\psi - \mathcal{P}_W\psi, w) = 0, \quad w \in W_h.$$

Recall that the approximation properties of the mixed spaces are described by l_V and l_W in (2.1)–(2.3). The following theorem (with a straightforward modification for the lower order term and the boundary conditions) can be found in [34, 31, 16, 8, 6, 7, 11].

THEOREM 8.1. *For the standard mixed method* (3.1.2) *or* (3.2.1) *on affine (and special boundary) elements,*

$$(8.1) \qquad \|\mathbf{u} - \mathbf{U}\|_0 \leq C(\|p\|_l + \|\mathbf{u}\|_l)\, h^l, \qquad\qquad 1 \leq l \leq l_V,$$

$$(8.2) \qquad \|p - P\|_0 \leq C(\|p\|_l + \|\mathbf{u}\|_l)\, h^l, \qquad\qquad 1 \leq l \leq l_W,$$

$$(8.3) \qquad \|\nabla \cdot (\mathbf{u} - \mathbf{U})\|_0 \leq C(\|p - P\|_0 + \|\nabla \cdot \mathbf{u}\|_l\, h^l), \quad 0 \leq l \leq l_W.$$

Moreover, if $l_W = l_V$,

$$(8.4) \qquad \|\mathcal{P}_W p - P\|_0 \leq C(\|p\|_l + \|\nabla \cdot \mathbf{u}\|_l + \|\mathbf{u}\|_{l+1/2}) \, h^{l+1}, \quad 1 \leq l \leq l_W,$$

and, if $l_W < l_V$,

$$(8.5) \quad \|\mathcal{P}_W p - P\|_0 \leq C \big\{ (\|p\|_{l_1} + \|\mathbf{u}\|_{l_1} + \|\nabla \cdot \mathbf{u}\|_{l_1}) \, h^{l_1 + \min\{l_W, 2\}}$$
$$+ (\|p\|_{\ell_2} + \|\mathbf{u}\|_{l_2+1/2}) \, h^{l_2+1} \big\}, \quad 1 \leq l_1 \leq l_W, \, 1 \leq l_2 \leq l_V,$$

where C depends on Ω, $\|\alpha\|_{0,\infty}$, $\|K\|_{0,\infty}$, and $\|K^{-1}\|_{0,\infty}$, and also on $\|\alpha\|_{1,\infty}$ in (8.4) or if $l_W < l_V$, on $\|K\|_{1,\infty}$ in (8.4) and (8.5), and on $\|\alpha\|_{2,\infty}$ in (8.5).

The next theorem (with a modification for the lower order term) can be found in [2] (cf. [10]).

THEOREM 8.2. *For the expanded mixed method (3.3.4) with $G = I$ on affine (and special boundary) elements,*

$$(8.6) \qquad \|\mathbf{u} - \mathbf{U}\|_0 + \|\tilde{\mathbf{u}} - \tilde{\mathbf{U}}\|_0 \leq C(\|p\|_{l+1} + \|\mathbf{u}\|_l) \, h^l, \quad 1 \leq l \leq l_V,$$

$$(8.7) \qquad \|p - P\|_0 \leq C(\|p\|_{l+1} + \|\mathbf{u}\|_l) \, h^l, \qquad\qquad 1 \leq l \leq l_W,$$

$$(8.8) \qquad \|\nabla \cdot (\mathbf{u} - \mathbf{U})\|_0 \leq C(\|p - P\|_0 + \|\nabla \cdot \mathbf{u}\|_l \, h^l), \quad 0 \leq l \leq l_W.$$

Moreover, if $l_W = l_V$,

$$(8.9) \qquad \|\mathcal{P}_W p - P\|_0 \leq C(\|p\|_{l+1} + \|\nabla \cdot \mathbf{u}\|_l + \|\mathbf{u}\|_{l+1/2}) \, h^{l+1}, \quad 1 \leq l \leq l_W,$$

and, if $l_W < l_V$,

$$(8.10) \quad \|\mathcal{P}_W p - P\|_0 \leq C \big\{ (\|p\|_{l_1+1} + \|\mathbf{u}\|_{l_1} + \|\nabla \cdot \mathbf{u}\|_{l_1}) \, h^{l_1 + \min\{l_W, 2\}}$$
$$+ (\|p\|_{l_2+1} + \|\mathbf{u}\|_{l_2+1/2}) \, h^{l_2+1} \big\}, \quad 1 \leq l_1 \leq l_W, \, 1 \leq l_2 \leq l_V,$$

where C depends on Ω, $\|\alpha\|_{0,\infty}$, $\|K\|_{0,\infty}$, and $\|K^{-1}\|_{0,\infty}$, and also on $\|\alpha\|_{1,\infty}$ in (8.9) or if $l_W < l_V$, on $\|K\|_{1,\infty}$ in (8.9) and (8.10), and on $\|\alpha\|_{2,\infty}$ in (8.10).

For the curved elements defined in Section 4, note that Lemma 4.2 and the fact that $(\varphi, \nabla \cdot \mathbf{u})_E = (J\hat{\varphi}, \widehat{\nabla \cdot \mathbf{u}})_{\hat{E}}$ implies

$$(8.11) \qquad\qquad \nabla \cdot \mathbf{u}(\mathbf{x}) = \widehat{\nabla \cdot \mathbf{u}} \circ F^{-1}(\mathbf{x}) = \left(\frac{1}{J} \hat{\nabla} \cdot \hat{\mathbf{u}} \right) \circ F^{-1}(\mathbf{x});$$

thus, in general $\nabla \cdot V_h \neq W_h$, unless the map F is piecewise affine.

THEOREM 8.3. *For the standard mixed method (3.1.2) or (3.2.1) on curved elements, the estimates (8.1)–(8.5) hold, and for the expanded mixed method (3.3.4) with $G = J^{-1} DF \, DF^T$ on curved elements, the estimates (8.6)–(8.10) hold, with the replacement of*

$$\|p\|_s, \quad \|\mathbf{u}\|_s, \quad and \quad \|\nabla \cdot \mathbf{u}\|_s,$$

by

$$C_{F,s} \|p\|_s, \quad C_{F,s+1} \|\mathbf{u}\|_s, \quad and \quad C_{F,s+1} \|\nabla \cdot \mathbf{u}\|_s,$$

respectively, for any $s \in \mathbf{R}$. Now C depends on

$$\hat{\Omega}, \quad \|\alpha\|_{0,\infty}, \quad \|J\|_{0,\infty}, \quad \|J^{-1}\|_{0,\infty}, \quad \|DF\|_{0,\infty},$$

$$\|DF^{-1}\|_{0,\infty}, \quad \|K\|_{0,\infty}, \quad and \quad \|K^{-1}\|_{0,\infty},$$

and also on $\|\alpha\|_{1,\infty}$ and $\|J\|_{1,\infty}$ in (8.4) and (8.9) or if $l_W < l_V$, on $\|K\|_{1,\infty}$, $\|DF\|_{1,\infty}$, and $\|DF^{-1}\|_{1,\infty}$ in the last two estimates of each method, and on $\|\alpha\|_{2,\infty}$ and $\|J\|_{2,\infty}$ in (8.5) and (8.10).

Proof. The results follow from Theorems 8.1 and 8.2 applied to the transformed problems (5.2) and (5.6), using relations (4.1.1), (4.1.2), and (8.11). $\quad\Box$

REMARK. Other known estimates in the H^{-s} and L^p norms for affine and special boundary elements [16, 6, 7, 20, 2] can also be transformed for curved elements by these techniques. As described in [27, 18, 19], if the grid is rectangular, RTN spaces are used, and K is a scalar or diagonal matrix in the standard mixed method, we have also super-convergence for the velocity error in a certain discrete norm (for RT_0, this is equivalent to the trapezoidal-midpoint rule applied to the L^2-norm). However, since the map introduces a non-diagonal transformation of K, these results do not carry over directly to curved elements.

REMARK. If multi-linear, quadrilateral and hexahedral elements are used, F is not continuous; however, we have approximation results because they hold element by element. If F is locally bilinear, then (see [34])

$$\|DF\|_{0,\infty} \leq C h^{-1} \quad and \quad \|DF\|_{j,\infty} \leq C h^{-2}, \quad j \geq 1,$$

and the results are non-optimal. However, for the Raviart-Thomas elements in two dimensions, Thomas [34] extracted the sharper estimates:

$$(8.28) \qquad \|\Pi\mathbf{u} - \mathbf{u}\|_0 \leq C(\|\mathbf{u}\|_j + h\|\nabla \cdot \mathbf{u}\|_j)h^j, \quad 1 \leq j \leq l_V,$$

$$(8.29) \qquad \|\nabla \cdot (\Pi\mathbf{u} - \mathbf{u})\|_{-s} \leq C(\|\nabla \cdot \mathbf{u}\|_{j-1} + h\|\nabla \cdot \mathbf{u}\|_j)h^{j-1+s},$$
$$0 \leq s \leq l_W, \; 1 \leq j \leq l_W.$$

These results lead to similar estimates (with $\pi\mathbf{u}$ replaced by $\mathbf{U}$) for the standard mixed method on quadrilateral and hexahedral elements. Moreover, similar results can be obtained for the expanded mixed method (without quadrature).

To describe the results for logically rectangular grids, we need some relatively standard cell-centered finite difference notation, given here in two dimensions for simplicity. Denote the grid points on $\hat{\Omega}$ by

$$(\hat{x}_{i+1/2}, \hat{y}_{j+1/2}), \quad i = 0, ..., N_{\hat{x}}, \; j = 0, ..., N_{\hat{y}},$$

and then define

$$\hat{x}_i = \tfrac{1}{2}(\hat{x}_{i+1/2} + \hat{x}_{i-1/2}), \quad i = 1, N_{\hat{x}},$$

$$\hat{y}_j = \tfrac{1}{2}(\hat{y}_{j+1/2} + \hat{y}_{j-1/2}), \quad j = 1, N_{\hat{y}}.$$

These points are mapped to points in Ω defined by the corresponding symbol without the caret. We write $\mathbf{v} = (v^x, v^y)$ for $\mathbf{v} \in \mathbf{R}^2$, and for any function $\hat{\psi}(\hat{x}, \hat{y})$, let

$\hat{\psi}_{ij}$ denote $\hat{\psi}(\hat{x}_i, \hat{y}_j)$, let $\hat{\psi}_{i+1/2,j}$ denote $\hat{\psi}(\hat{x}_{i+1/2}, \hat{y}_j)$, etc., with a similar definition for functions and points without carets.

For $w \in W \cap C^0(\bar{\Omega})$ and $\mathbf{v} \in \tilde{V} \cap (C^0(\bar{\Omega}))^d$ let

$$\|w\|_{\mathbf{M}}^2 = (w, w)_{\mathbf{M}}, \quad \|\mathbf{v}\|_{\mathbf{TM}}^2 = (\mathbf{v}, \mathbf{v})_{\mathbf{TM}}, \quad \text{and} \quad \|\mathbf{v}\|_{\mathbf{M}}^2 = (\mathbf{v}, \mathbf{v})_{\mathbf{M}};$$

these can also be defined on W_h or $\tilde{V}_h$. On W_h and V_h, the first two are norms, and the third is a semi-norm. For $E = E_{ij} \in \mathcal{E}_h$, define

$$\|\mathbf{v}\|_{\nu,E}^2 = \left[(\mathbf{v} \cdot \nu)_{i-1/2,j}^2 + (\mathbf{v} \cdot \nu)_{i+1/2,j}^2 + (\mathbf{v} \cdot \nu)_{i,j-1/2}^2 + (\mathbf{v} \cdot \nu)_{i,j+1/2}^2 \right] |E|,$$

$$\|\mathbf{v}\|_\nu^2 = \sum_E \|\mathbf{v}\|_{\nu,E}^2,$$

where ν is the unit normal vector to the edges of the elements; this is a norm on V_h.

The following definition concerning mesh refinement is needed for the next two results (cf. [2]).

DEFINITION 8.4. *For $\ell \geq 1$, an asymptotic family of meshes is said to be generated by a C^ℓ map if each mesh is an image by a fixed map F of a mesh that is composed of standard, regular reference elements. Here F must be in $C^\ell(\overline{\hat{\Omega}})$ with $J > 0$.*

THEOREM 8.5. *For the cell-centered finite difference method on a logically rectangular grid (5.6c)–(5.6d), (6.1), if $p \in C^{3,1}(\bar{\Omega})$, $\mathbf{u} \in \left(C^1(\bar{\Omega}) \cap W^{2,\infty}(\Omega) \right)^d$, and $K \in \left(C^1(\bar{\Omega}) \cap W^{2,\infty}(\Omega) \right)^{d \times d}$, then there exists a constant $C_{F,3}$, independent of h but dependent on the solution, K, and F as indicated, such that*

$$(8.12) \qquad \|\mathbf{u} - \mathbf{U}\|_{\mathbf{M}} + \|\tilde{\mathbf{u}} - \tilde{\mathbf{U}}\|_{\mathbf{M}} \leq C_{F,3} h^r,$$

$$(8.13) \qquad \|\mathbf{u} - \mathbf{U}\|_\nu + \|\tilde{\mathbf{u}} - \tilde{\mathbf{U}}\|_\nu \leq C_{F,3} h^r,$$

$$(8.14) \qquad \|\nabla \cdot (\mathbf{u} - \mathbf{U})\|_{\mathbf{M}} \leq C_{F,3} h^2,$$

$$(8.15) \qquad \|p - P\|_{\mathbf{M}} \leq C_{F,3} h^2,$$

where $r = 2$ if $\mathcal{K}$ in (5.7) is diagonal and $\Gamma^D = \emptyset$ and $r = 3/2$ otherwise.

Proof. This theorem is the transformation of the results of [2; Theorems 5.6 and 5.8]. To prove (8.12), we write

$$\|\mathbf{u} - \mathbf{U}\|_{\mathbf{M}}^2 = \left\| J^{-1} DF(\hat{\mathbf{u}} - \hat{\mathbf{U}}) \right\|_{\mathbf{M}}^2 \leq C \|\hat{\mathbf{u}} - \hat{\mathbf{U}}\|_{\mathbf{M}}^2.$$

Now

$$\|\hat{u}^x - \hat{u}_h^x\|_{\mathbf{M}}^2 = \sum_{\hat{E}} (\hat{u}^x - \hat{u}_h^x)_{ij}^2 |\hat{E}|$$

$$\leq \sum_{\hat{E}} \left\{ \frac{1}{2} \left[(\hat{u}^x - \hat{u}_h^x)_{i-1/2,j} + (\hat{u}^x - \hat{u}_h^x)_{i+1/2,j} \right] + C\hat{h}^2 \right\}^2 |\hat{E}|$$

$$\leq C \left(\|\hat{\mathbf{u}} - \hat{\mathbf{u}}_h\|_{\mathbf{TM}}^2 + \|\hat{\mathbf{u}} - \hat{\mathbf{u}}_h\|_{\mathbf{TM}} \hat{h}^2 + \hat{h}^4 \right) \leq C_{F,3} h^{2r},$$

using a result from [2] for the last inequality. A similar bound for $\|\hat{u}^y - \hat{u}_h^y\|_{\mathbf{M}}$ completes the proof of (8.12). Estimate (8.13) follows trivially from the bound of $\|\hat{\mathbf{u}} - \hat{\mathbf{U}}\|_{\mathbf{TM}}$ in [2] and the fact that $\mathbf{v} \cdot \nu = J_{\hat{\nu}}^{-1} \hat{\mathbf{v}} \cdot \hat{\nu}$ for $\mathbf{v} \in V$. To prove (8.14), we observe that $\hat{\nabla} \cdot \hat{\mathbf{U}} = \mathcal{P}_{\hat{W}} \hat{\nabla} \cdot \hat{\mathbf{u}}$ implies

$$\|\hat{\nabla} \cdot (\hat{\mathbf{u}} - \hat{\mathbf{U}})\|_{\mathbf{M}} \leq C\|\hat{\nabla} \cdot \hat{\mathbf{u}}\|_2 \hat{h}^2,$$

and, since $\widehat{\nabla \cdot \mathbf{u}} = J^{-1} \hat{\nabla} \cdot \hat{\mathbf{u}}$,

$$\|\nabla \cdot (\mathbf{u} - \mathbf{U})\|_{\mathbf{M}} \leq C\|\hat{\nabla} \cdot (\hat{\mathbf{u}} - \hat{\mathbf{U}})\|_{\mathbf{M}} \leq C_{F,3} h^2.$$

Finally, (8.15) follows from the estimate $\|\mathcal{P}_{\hat{W}} \hat{p} - \hat{P}\|_0 \leq C\hat{h}^2$ proven in [2]. $\quad\square$

REMARK. The above results imply L^2 super-convergence for the computed pressure, velocity, and its divergence at the midpoints of the elements. The normal component of the velocity at the midpoints of the edges or faces is also super-convergent. Moreover, full second order super-convergence of the velocities is obtained in the strict interior of the domain [2; Theorem 5.10].

THEOREM 8.6. *For the triangular cell-centered finite difference method (5.6c)–(5.6d), (7.2), if the computational grid is generated by a C^3 map, then*

$$\|\mathbf{u} - \mathbf{U}\|_0 + \|\tilde{\mathbf{u}} - \tilde{\mathbf{U}}\|_0 \leq C_{F,3} h,$$
$$\|p - P\|_0 \leq C_{F,3} h,$$
$$\|\nabla \cdot (\mathbf{u} - \mathbf{U})\|_0 \leq C_{F,3} h.$$

Proof. This result is new, and we need some notation for its proof. Assume the grid consists of equilateral triangles; the general case follows for curved elements as previously. Let

$$E_Q(\psi) = \sum_{T \in \mathcal{E}_h} \left[\int_T \psi \, dx - Q_T(\psi) \right]$$

denote the quadrature error. It is well known [15] that

(8.16) $$|E_Q(\psi)| \leq \sum_{T \in \mathcal{E}_h} \sum_{i,j} \int_T \left| \frac{\partial^2 \psi}{\partial x_i \partial x_j} \right| dx \, h^2.$$

If $\mathbf{q} \in (H^2(\Omega))^d$ and $\mathbf{v} \in V_h$, then $\mathbf{v}$ is piecewise linear and

(8.17) $$|E_Q(\mathbf{q} \cdot \mathbf{v})| \leq \sum_{T \in \mathcal{E}_h} \sum_{i,j} \int_T \left(\left| \frac{\partial^2 \mathbf{q}}{\partial x_i \partial x_j} \cdot \mathbf{v} \right| + \left| \frac{\partial \mathbf{q}}{\partial x_i} \cdot \frac{\partial \mathbf{v}}{\partial x_j} \right| \right) dx \, h^2$$
$$\leq C\|\mathbf{q}\|_2 \|\mathbf{v}\|_1 h^2 \leq C\|\mathbf{q}\|_2 \|\mathbf{v}\|_0 h,$$

by an inverse inequality [12].

We denote by $\mathcal{Q}_V : (L^2(\Omega))^d \to V_h$ the discrete $(L^2)^d$-projection operator defined by

$$\sum_{T \in \mathcal{E}_h} Q_T((\mathcal{Q}_V \mathbf{q} - \mathbf{q}) \cdot \mathbf{v}) = 0, \quad \mathbf{v} \in V_h.$$

Clearly [15],

$$(8.18) \qquad \|\mathcal{Q}_V \mathbf{q} - \mathbf{q}\|_0 \leq C \|\mathbf{q}\|_1 \, h.$$

Let $\pi : (H^1(\Omega))^d \to V_h$ be the projection [31, 16] defined by

$$\sum_{E \in \mathcal{E}_h} \langle (\pi \mathbf{q} - \mathbf{q}) \cdot \nu, \mu \rangle_{\partial E} = 0, \quad \mu \in \Lambda_h.$$

By the divergence theorem, $(\nabla \cdot (\pi \mathbf{q} - \mathbf{q}), w) = 0$ for $w \in W_h$, and approximation theory gives that

$$(8.19) \qquad \|\pi \mathbf{q} - \mathbf{q}\|_0 \leq C \|\mathbf{q}\|_1 \, h,$$
$$(8.20) \qquad \|\nabla \cdot (\pi \mathbf{q} - \mathbf{q})\|_0 \leq C \|\nabla \cdot \mathbf{q}\|_1 \, h.$$

Let $\mathcal{P}_\Lambda : L^2 \to \Lambda_h^N$ denote the L^2 projection defined by

$$\langle \mathcal{P}_\Lambda \varphi - \varphi, \mu \rangle_{\Gamma^N} = 0, \quad \mu \in \Lambda_h^N.$$

Easily, the L^2-projection errors are

$$(8.21) \qquad \|\mathcal{P}_\Lambda \varphi - \varphi\|_{0,\Gamma^N} \leq C \|\varphi\|_{H^1(\Gamma^N)} \, h,$$
$$(8.22) \qquad \|\mathcal{P}_W \psi - \psi\|_0 \leq C \|\psi\|_1 \, h.$$

For simplicity assume α is constant; the variable coefficient case follows as a slight perturbation of the proof in the standard way. Subtracting the weak form of the problem, (3.3.3) with $G = I$, from the discrete method, (5.6c)–(5.6d), (7.2) with F as the identity mapping, and inserting our projections operators gives

$$(8.23a) \qquad \sum_{T \in \mathcal{E}_h} Q_T((\mathbf{U} - \mathcal{Q}_V \mathbf{u}) \cdot \tilde{\mathbf{v}})$$
$$= (K(\tilde{\mathbf{U}} - \tilde{\mathbf{u}}), \tilde{\mathbf{v}}) + E_Q(\mathbf{u} \cdot \tilde{\mathbf{v}}), \qquad \tilde{\mathbf{v}} \in V_h,$$
$$(8.23b) \qquad \sum_{T \in \mathcal{E}_h} Q_T((\tilde{\mathbf{U}} - \mathcal{Q}_V \tilde{\mathbf{u}}) \cdot \mathbf{v}) - (P - \mathcal{P}_W p, \nabla \cdot \mathbf{v})$$
$$= -\langle \lambda - \mathcal{P}_\Lambda p, \mathbf{v} \cdot \nu \rangle_{\Gamma^N} + E_Q(\tilde{\mathbf{u}} \cdot \mathbf{v}), \qquad \mathbf{v} \in V_h,$$
$$(8.23c) \qquad (\alpha(P - \mathcal{P}_W p), w) + (\nabla \cdot (\mathbf{U} - \pi \mathbf{u}), w) = 0, \qquad w \in W_h,$$
$$(8.23d) \qquad \langle (\mathbf{U} - \pi \mathbf{u}) \cdot \nu, \mu \rangle_{\Gamma^N} = 0, \qquad \mu \in \Lambda_h^N.$$

Take $\tilde{\mathbf{v}} = \tilde{\mathbf{U}} - \mathcal{Q}_V \tilde{\mathbf{u}}$, $\mathbf{v} = \mathbf{U} - \pi \mathbf{u}$, $w = P - \mathcal{P}_W p$, and $\mu = \lambda - \mathcal{P}_\Lambda p$. A combination of the resulting equations yields

$$(\alpha(P - \mathcal{P}_W p), P - \mathcal{P}_W p) + (K(\tilde{\mathbf{U}} - \mathcal{Q}_V \tilde{\mathbf{u}}), \tilde{\mathbf{U}} - \mathcal{Q}_V \tilde{\mathbf{u}})$$
$$= E_Q(\tilde{\mathbf{u}} \cdot (\mathbf{U} - \pi \mathbf{u})) - E_Q(\mathbf{u} \cdot (\tilde{\mathbf{U}} - \mathcal{Q}_V \tilde{\mathbf{u}})) + (K(\tilde{\mathbf{u}} - \mathcal{Q}_V \tilde{\mathbf{u}}), \tilde{\mathbf{U}} - \mathcal{Q}_V \tilde{\mathbf{u}})$$
$$+ \sum_{T \in \mathcal{E}_h} Q_T((\tilde{\mathbf{U}} - \mathcal{Q}_V \tilde{\mathbf{u}}) \cdot (\pi \mathbf{u} - \mathcal{Q}_V \mathbf{u})).$$

Since $\{\sum_{T \in \mathcal{E}_h} Q_T(\mathbf{v} \cdot \mathbf{v})\}^{1/2}$ is equivalent to the L^2-norm for $\mathbf{v} \in V_h$, standard estimates, (8.17), and (8.18) allow us to conclude that

$$(8.24) \qquad \|\sqrt{\alpha}(P - \mathcal{P}_W p)\|_0 + \|\tilde{\mathbf{U}} - \mathcal{Q}_V \tilde{\mathbf{u}}\|_0$$
$$\leq C\{[\|\tilde{\mathbf{u}}\|_2 + \|\mathbf{u}\|_2]\, h + \|\pi\mathbf{u} - \mathcal{Q}_V \mathbf{u}\|_0\} + \epsilon\|\mathbf{U} - \pi\mathbf{u}\|_0$$

for any $\epsilon > 0$. If we take $\tilde{\mathbf{v}} = \mathbf{U} - \mathcal{Q}_V \mathbf{u}$ in (8.23a), then

$$\sum_{T \in \mathcal{E}_h} Q_T((\mathbf{U} - \mathcal{Q}_V \mathbf{u}) \cdot (\mathbf{U} - \mathcal{Q}_V \mathbf{u})) = (K(\tilde{\mathbf{U}} - \tilde{\mathbf{u}}), \mathbf{U} - \mathcal{Q}_V \mathbf{u}) + E_Q(\mathbf{u} \cdot (\mathbf{U} - \mathcal{Q}_V \mathbf{u})),$$

and so

$$(8.25) \qquad \|\mathbf{U} - \mathcal{Q}_V \mathbf{u}\|_0 \leq C\{\|\mathbf{u}\|_2\, h + \|\tilde{\mathbf{U}} - \tilde{\mathbf{u}}\|_0\}.$$

If we take $w = \nabla \cdot (\mathbf{U} - \pi\mathbf{u})$ in (8.23c) and manipulate the expression as above, then

$$(8.26) \qquad \|\nabla \cdot (\mathbf{U} - \pi\mathbf{u})\|_0 \leq C\|\sqrt{\alpha}(P - \mathcal{P}_W p)\|_0.$$

Finally, let $\mathbf{v} \in V_h$ be chosen such that for some ψ,

$$\nabla \cdot \mathbf{v} = P - \mathcal{P}_W p - \mathcal{P}_W(\alpha\psi),$$
$$\|\psi\|_0 + \|\mathbf{v}\|_0 \leq C\|P - \mathcal{P}_W p\|_0,$$
$$\mathbf{v} \cdot \nu = 0 \quad \text{on } \Gamma^N.$$

Such a $\mathbf{v}$ exists [31, 16]; for example, solve

$$\alpha\psi - \nabla \cdot K\nabla\psi = P - \mathcal{P}_W p \quad \text{in } \Omega,$$
$$\psi = 0 \qquad\qquad\qquad\quad \text{on } \Gamma^D,$$
$$K\nabla\psi \cdot \nu = 0 \qquad\qquad\quad \text{on } \Gamma^N,$$

and then define $\mathbf{v} = -\pi K\nabla\psi$ which preserves the normal flux and divergence of $-K\nabla\psi$ by the properties of π, and bounds the norms by approximation and elliptic regularity theory. This $\mathbf{v}$ in (8.23b) gives

$$(8.27) \qquad \|P - \mathcal{P}_W p\|_0 \leq C\{\|\tilde{\mathbf{u}}\|_2\, h + \|\tilde{\mathbf{U}} - \mathcal{Q}_V \tilde{\mathbf{u}}\|_0 + \|\sqrt{\alpha}(P - \mathcal{P}_W p)\|_0\}.$$

The theorem follows from the approximation properties of the projections and (8.24)–(8.27). $\quad\square$

REMARK. Experimentally we find that for smooth problems p is $O(h^2)$ super-convergent at the centroids of the triangles. Moreover, on three-lines meshes, the normal fluxes are also $O(h^2)$ super-convergent [17].

9. Computational results. We present some numerical results that illustrate the theory by solving elliptic problems in two and three dimensions. The results come from two different computer codes, one implemented to solve the problem on a logically rectangular grid, and the other implemented to use more general meshes.

9.1. Logically rectangular. The logically rectangular code was developed initially as a rectangular code following the ideas of [2] to treat tensors. A preprocessor was added to modify the coefficients of the problem as described in §§5–6 above, and a postprocessor was added to transform the reference solution $(\hat{P}, \hat{\mathbf{U}})$ to the solution $(P, \mathbf{U})$ on the physical domain.

In our examples, the true domain Ω is defined as the image of the unit square by a given smooth map F. A uniform, rectangular grid on $\hat{\Omega}$ and the map define our curved grid on Ω. The derivatives of the map, needed for the computations, are evaluated numerically, using only the coordinates of the grid points. We test diagonal and full permeability tensors. Note that the problem on the computational domain always has a full tensor (see (5.7)), unless the permeability K is isotropic and the map is orthogonal. In the following examples the permeability is

$$K = K_D = \begin{pmatrix} 10 & 0 \\ 0 & 1 \end{pmatrix} \quad \text{or} \quad K = K_F = \begin{pmatrix} (x+2)^2 + y^2 & \sin(xy) \\ \sin(xy) & 1 \end{pmatrix},$$

and the true solution is

$$p(x, y) = x^3 y + y^4 + \sin(x)\cos(y),$$

with f defined accordingly by (1.1), and (1.1c) or (1.1d) replaced by the proper boundary condition (both Dirichlet and Neumann conditions were tested). The map is

$$\begin{pmatrix} x \\ y \end{pmatrix} = F\begin{pmatrix} \hat{x} \\ \hat{y} \end{pmatrix} = \begin{pmatrix} \hat{x} + \frac{1}{10}\cos(3\hat{y}) \\ \hat{y} + \frac{1}{10}\sin(6\hat{x}) \end{pmatrix}.$$

The problem is shown in Figure 9.1.

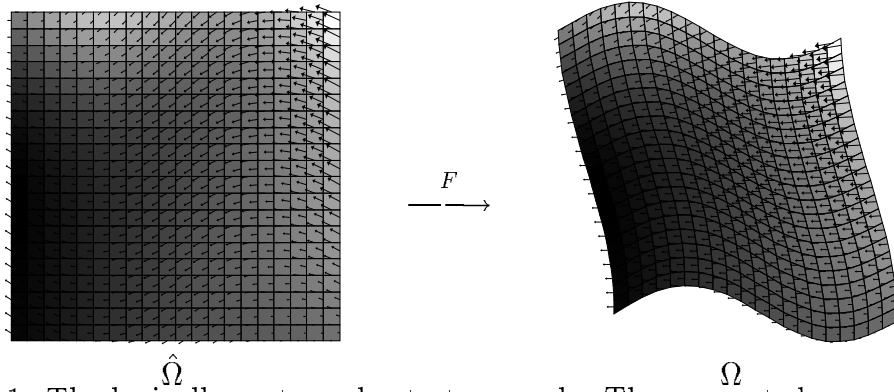$\hat{\Omega}$ $\xrightarrow{\;F\;}$ Ω

Fig. 9.1. *The logically rectangular test example. The computed pressure and velocity are shown for the case using K_F with Dirichlet boundary conditions on both the computational and true domains.*

Convergence rates for the test cases are given in Table 9.1. The rates were established by running the test case for 6 levels of grid refinement. We assume the error has the form Ch^α and compute C and α by a least squares fit to the data. As can be seen, the pressures and velocities are super-convergent to the true solution in the discrete norms. This verifies (8.15) and (8.12) with $r = 3/2$.

Table 9.1. Discrete norm convergence rates for the logically rectangular test example: $\|P - p\|_{\mathbf{M}} \leq C_p\, h^{\alpha_p}$ and $\|\mathbf{U} - \mathbf{u}\|_{\mathbf{M}} \leq C_u\, h^{\alpha_u}$.

Tensor	Boundary Condition	C_p	α_p	C_u	α_u
K_D	Dirichlet	0.417	2.260	0.588	1.659
K_D	Neumann	7.380	2.138	0.466	1.633
K_F	Dirichlet	0.435	2.205	0.611	1.710
K_F	Neumann	10.09	2.130	0.648	1.754

9.2. General meshes. The second code, called the Rice Unstructured Flow (RUF) Code [23], is written in C++ for flexibility and implements a variety of mixed method formulations on a wide variety of two and three dimensional meshes composed of triangular, quadrilateral, tetrahedral, and hexahedral elements. This code operates element-by-element, and thus we approximate the map F locally by affine or bi/tri-linear mappings, as mentioned in §7.

We created a large suite of test problems that we used to examine the behavior of the numerical methods described above. In each case the boundary conditions and the forcing term were constructed to match the prescribed solution. We report in detail on a typical case and then summarize the results from the full test suite.

A typical case. Among the domains considered was that shown in Figure 9.2. This figure illustrates the initial decomposition of the domain into elements.
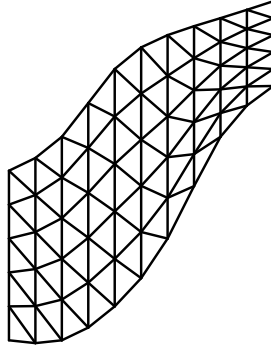

Fig. 9.2. The mesh for a typical example.

In the convergence study, the domain was described by cubic splines, which were used to generate progressively finer meshes directly. The resulting family of meshes satisfies the definition of smoothness given in Definition 8.4.

In Tables 9.2–9.3 we give detailed results for a test problem using Dirichlet boundary conditions,

$$(9.2.1) \qquad\qquad K = \begin{pmatrix} 1 & 0.5 \\ 0.5 & 3 \end{pmatrix},$$

and with the analytic solution

$$(9.2.2) \qquad p(x,y) = 1 - 2.1\cos y + 3.1\cos 2y + 4\cos 3y$$
$$+ \cos x(5 + 6.2\cos y - 7.1\cos 2y + 8\cos 3y)$$
$$+ \cos 2x(9 - 10\cos y + 1.1\cos 2y + 12\cos 3y).$$

We report errors in the pressure and velocity approximations for both the mixed method implemented directly and the cell-centered finite difference approximation described in §§5–7. As can be seen, the mixed and cell-centered methods are equally accurate, and converge at the expected rate.

Table 9.2. The pressure error $\|P - p\|_{\mathbf{M}}$ for a typical example.

h	Mixed	Cell-centered
0.1	0.09366	0.09648
0.05	0.02577	0.02422
0.025	0.00668	0.00608
Rate	h^2	h^2

Table 9.3. The velocity error $\|\mathbf{U} - \mathbf{u}\|_{\mathbf{M}}$ for a typical example.

h	Mixed	Cell-centered
0.1	5.70698	5.92678
0.05	2.93120	2.97586
0.025	1.47783	1.48691
Rate	h	h

Summary of the test suite. We conducted approximately 200 experiments with RUF, varying the domain, the shape of the elements, the type of mesh refinement used, the test equation, and the tensor K. We summarize results for smooth meshes that contain no tetrahedra, since non-smooth meshes and tetrahedral elements degrade the convergence rates; we discuss these exceptional cases in the next section.

In all smooth cases, the error in the pressure converged approximately like $O(h^2)$ for the mixed method (or the equivalent hybrid form) and the cell-centered finite difference method. Similarly the error in the flux converged at least as well as $O(h)$ (grids of quadralaterals or hexahedra perform better, as noted above).

For most methods and test cases, the condition number of the linear system was $O(h^{-2})$, as estimated by the number of conjugate gradient iterations used. Using a conjugate gradient solver with no preconditioning, the mixed method implemented as a saddle point problem took much longer than the cell-centered finite difference method (approximately 50 times longer on 2000 elements). On typical smooth mesh problems, the cell-centered finite difference method took approximately half as much CPU time as the face-centered, hybrid method.

On rectangles one finds that the velocities are super-convergent at special points and can be post-processed to yield second order accurate vector approximations everywhere. A new post processing scheme developed by the third author recovers extra accuracy for the velocities on triangular meshes as well [24]. The post-processing method can be applied to any of the mixed method variants. The convergence rate for the post processed flux is generally between $h^{1.5}$ and h^2, depending in part on the smoothness of the mesh refinement process. This and other related post-processing schemes are analyzed in [17], where it is shown that they recover second order accurate velocity fields on three-lines meshes. Moreover, although the resulting velocity fields do not conserve mass exactly, a special postprocessor choice makes the mass conservation errors extra small.

10. Non-smooth meshes and tensors and the enhanced finite difference method. In this section we discuss mesh smoothness and refinement processes and their impact on the accuracy of the cell-centered finite difference method. In Definition 8.4 we stated the requirements for a family of meshes to be smooth. A mesh refinement process is called *hierarchical* if an initial coarse mesh is refined using a smooth refinement process inside each of the original coarse elements. That is, the meshes form a smooth family within each coarse element, but not necessarily as a whole. (This type of mesh is a special example of a multi-block mesh.) In practice, most applications can use meshes and refinement schemes that can be classified as either smooth or hierarchical.

We observed numerically that the accuracy of our cell-centered finite difference approach breaks down on non-smooth meshes, or equivalently when K is not smooth. This is due to the fact that if F (or K) is not smooth, then the matrix $\mathcal{K}$ (see (5.7)) is not smooth. In this case, the convergence theory of §8 breaks down. We demonstrate this by two simple but typical examples. First consider the two triangle mesh shown in Figure 10.1. Using Dirichlet boundary conditions and taking the true solution $p(x, y) = y$, the usual mixed method reproduces p at the centroids of the triangles and **u** exactly, as it must for $O(h)$ order accuracy. The cell-centered finite difference method, in contrast, fails to compute either function correctly; for instance it yields $P = 0.35714$ instead of 0.33333.
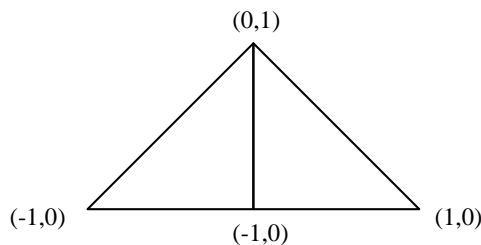

Fig. 10.1. A non-smooth mesh.

Figure 10.2 shows the error $P - p$ for a second example on a much finer mesh constructed from applying uniform refinement to an original coarse mesh of two dissimilar triangles. Darker shades indicate larger errors. Within each of the original
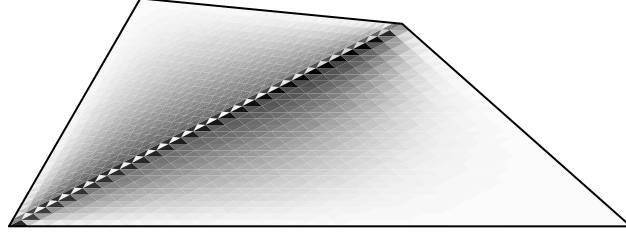
Fig. 10.2. *Error in* $P - p$ *on a hierarchically refined mesh using cell-centered finite differences.*

triangles, the mesh is smooth; the jump in DF across the central line produces the error pattern shown, somewhat like an artificial source term.

Since the normal component of $\hat{\mathbf{u}} = -\mathcal{K}\hat{\nabla}\hat{p}$ is continuous across interfaces, $\hat{\tilde{\mathbf{u}}}$ must be discontinuous across the interface where DF changes discontinuously; however, in the cell-centered finite difference method presented here, $\hat{\tilde{\mathbf{u}}}$ is approximated by a function $\hat{\tilde{\mathbf{U}}} \in V_h$ that is constrained to have continuous normal components across interfaces. We now relax this continuity requirement across element edges or faces for which DF is not smooth by enlarging $\tilde{V}_h$, and we call the resulting method the enhanced cell-centered finite difference method. It is enhanced in that we add face centered, Lagrange multiplier pressures on such element edges or faces, to maintain ease of solution. That is, we also enlarge V_h so that $V_h = \tilde{V}_h$ and A_2 in (3.3.6) remains square and invertible. For the problem of Figure 10.1, as we refine the mesh, we add Lagrange multipliers only on the line segment between the two coarse triangles. It gives the exact solution in the case of linear p.

In order to precisely formulate the basic idea of the enhanced method, consider a domain Ω consisting of just two regions Ω_1 and Ω_2 separated by an interface Γ^I, such as that shown in Figure 10.3. A weak form of (1.1), analogous to (3.3.3), can be defined by integrating over each Ω_i and summing. The result is (3.3.3a), (3.3.3d), and

$$(10.1a) \quad (G^{-1}\tilde{\mathbf{u}}, \mathbf{v}) - \sum_{i=1}^{2} (p, \nabla \cdot \mathbf{v})_{\Omega_i}$$

$$= -\langle g^D, \mathbf{v} \cdot \nu \rangle_{\Gamma^D} - \langle p, \mathbf{v} \cdot \nu \rangle_{\Gamma^N}$$

$$- \langle p, \mathbf{v} \cdot \nu_1 \rangle_{\Gamma^I} - \langle p, \mathbf{v} \cdot \nu_2 \rangle_{\Gamma^I}, \quad \mathbf{v} \in H(\mathrm{div};\Omega_1) \cup H(\mathrm{div};\Omega_2),$$

$$(10.1b) \quad (\alpha p, w) + \sum_{i=1}^{2} (\nabla \cdot \mathbf{u}, w)_{\Omega_i} = (f, w), \quad w \in L^2(\Omega),$$

$$(10.1c) \quad \langle \mathbf{u} \cdot \nu_1, \mu \rangle_{\Gamma^I} + \langle \mathbf{u} \cdot \nu_2, \mu \rangle_{\Gamma^I} = 0, \quad \mu \in H^{1/2}(\Gamma^I),$$

where $\mathbf{v} \cdot \nu_i$ means the normal component as defined from Ω_i. Note that (10.1c) insures continuity of flux across Γ^I.

We construct a finite element partition of Ω, where DF is smooth in Ω_1 and Ω_2 but not necessarily smooth along Γ^I. Let $\mathcal{E}_h^k$ denote a finite element partition of Ω_k, $k = 1, 2$, and let $\mathcal{E}_h = \mathcal{E}_h^1 \cup \mathcal{E}_h^2$. Assume that $\mathcal{E}_h^1$ and $\mathcal{E}_h^2$ match at the edge
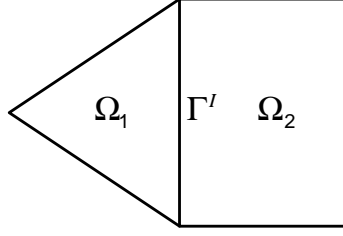
Fig. 10.3. *Domain decomposition.*

Γ^I, so that $\mathcal{E}_h$ is a valid partition of the whole domain Ω. Let $V_h^k \subset H(\text{div}; \Omega_k)$, $W_h^k \subset L^2(\Omega_k)$ denote the RT_0 spaces on $\mathcal{E}_h^k$, $k = 1, 2$. Let $V_h^* = V_h^1 \cup V_h^2 \subset \bar{V}_h$, $\tilde{V}_h^* = \tilde{V}_h^1 \cup \tilde{V}_h^2 \supset V_h^*$, and $W_h = W_h^1 \cup W_h^2$. Let $\Lambda_h^I \in L^2(\Gamma^I)$ denote the restriction to Γ^I of the space Λ_h. Then the enhanced method seeks $\mathbf{U} \in V_h^*$, $\tilde{\mathbf{U}} \in \tilde{V}_h^*$, $P \in W_h$, and $\lambda \in \Lambda_h^N \cup \Lambda_h^I$ satisfying

(10.2a)
$$(G^{-1}\mathbf{U}, \tilde{\mathbf{v}}) = (G^{-1}KG^{-1}\tilde{\mathbf{U}}, \tilde{\mathbf{v}}), \qquad \tilde{\mathbf{v}} \in \tilde{V}_h^*,$$

(10.2b)
$$(G^{-1}\tilde{\mathbf{U}}, \mathbf{v}) - \sum_{i=1}^{2}(P, \nabla \cdot \mathbf{v})_{\Omega_i}$$
$$= -\langle g^D, \mathbf{v} \cdot \nu \rangle_{\Gamma^D} - \langle \lambda, \mathbf{v} \cdot \nu \rangle_{\Gamma^N}$$
$$\quad - \langle \lambda, \mathbf{v} \cdot \nu_1 \rangle_{\Gamma^I} - \langle \lambda, \mathbf{v} \cdot \nu_2 \rangle_{\Gamma^I}, \quad \mathbf{v} \in V_h^*,$$

(10.2c)
$$(\alpha P, w) + \sum_{i=1}^{2}(\nabla \cdot \mathbf{U}, w)_{\Omega_i} = (f, w), \quad w \in W_h,$$

(10.2d)
$$\langle \mathbf{U} \cdot \nu, \mu \rangle_{\Gamma^N} = \langle g^N, \mu \rangle_{\Gamma^N}, \qquad \mu \in \Lambda_h^N,$$

(10.2e)
$$\langle \mathbf{U} \cdot \nu_1, \mu \rangle_{\Gamma^I} + \langle \mathbf{U} \cdot \nu_2, \mu \rangle_{\Gamma^I} = 0 \qquad \mu \in \Lambda_h^I.$$

We further take $\tilde{V}_h^* = V_h^*$ and approximate the appropriate integrals by quadrature to obtain the enhanced cell-centered finite difference method. The linear system can be easily reduced to a symmetric, positive definite system for the pressures P and λ alone.

We illustrate the enhanced finite difference method on a typical example posed on the domain shown in Fig. 10.4, where the initial decomposition of the domain into coarse elements is also shown. The domain is neither simply connected nor convex; moreover, we chose to use both rectangles and triangles. The domain was refined uniformly to generate progressively finer meshes. Refinement means replacing each triangle or rectangle with 4 smaller but geometrically similar ones. The finest mesh had 2432 elements. Uniform refinement generates hierarchical meshes: each new mesh contains all the edges of the previous one. However, the geometry mapping is clearly not smooth across edges of the original coarse mesh.

In Tables 10.1 and 10.2, we give results for a test problem using Dirichlet boundary conditions, K defined by (9.2.1), and true solution (9.2.2). This non-smooth, hierarchical example shows that indeed the cell-centered finite difference method loses accuracy (about one half power of h in this example, but in other
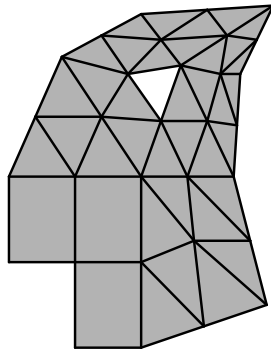
Fig. 10.4. A non-smooth mesh example.

examples even more) in both pressure and flux as compared to the standard mixed method; however, there is no loss in accuracy for the enhanced finite difference method. Moreover, if instead of this hierarchical refinement procedure, we use a smooth procedure, then the cell-centered finite difference method achieves the same convergence orders as the other methods. Thus, it is the non-smooth mesh alone that causes degradation of convergence.

Table 10.1. The pressure error $\|P - p\|_{\mathbf{M}}$ for a hierarchical example.

h	Mixed	Cell-centered	Enhanced
0.16	0.39	0.48	0.59
0.08	0.11	0.12	0.11
0.04	0.029	0.043	0.026
0.02	0.0076	0.019	0.0062
Rate	h^2	$h^{1.4}$	h^2

Table 10.2. The velocity error $\|\mathbf{U} - \mathbf{u}\|_{\mathbf{M}}$ for a hierarchical example.

h	Mixed	Cell-centered	Enhanced
0.16	6.0	9.3	6.4
0.08	3.1	5.9	3.5
0.04	1.5	3.7	1.6
0.02	0.77	2.5	0.80
Rate	h	$h^{0.6}$	h

We also considered the enhanced method and non-smooth meshes in the test suite of 200 problems run with RUF. The error in the pressure converged approximately like $O(h^2)$ for all methods, including the enhanced method, except in the case of the cell-centered finite difference method on non-smooth meshes. Similarly the error in the flux converged at least as well as $O(h)$ for all methods, again except for the cell-centered method on non-smooth meshes. Thus, indeed, the enhanced method corrects the cell-centered method in the presence of non-smooth meshes. Moreover, on hierarchical meshes that have coarse blocks with smooth, logically rectangular meshes, the enhanced method achieved the usual super-convergence.

Recall that we used a conjugate gradient solver with no preconditioning. Generally, the enhanced method was somewhat slower than the hybrid method on coarse meshes, since it solves for both pressures and Lagrange multipliers. But by around four levels of mesh refinement the two methods took the same amount of time to solve, since the enhanced method does not need Lagrange multipliers on every edge. The enhanced method outperforms the hybrid method when additional refinement is used.

In the hybrid method, Lagrange multiplier pressures are introduced on the boundary of every element in $\mathcal{E}_h$. In many cases, Lagrange multipliers are only needed on the boundaries of a few elements, as above. A similar situation arises when applying the domain decomposition techniques described in [22], where Lagrange multipliers are introduced only on the element faces between sub-domains. In the enhanced method, the multipliers are needed to preserve accuracy of the numerical solution; however, as a side effect, they can be used to introduce parallelism into the solution process. The resulting linear system for the pressures can be further reduced to an equation for Lagrange pressures alone. In [22, 21, 14, 13], various methods for solving such a system on parallel computers are developed and analyzed.

We close this section by returning to tetrahedral meshes. Since regular tetrahedra do not fill space (whereas equilateral triangles do tile the plane), tetrahedral meshes unavoidably produce discontinuous $\mathcal{K}$ everywhere, no matter how much one attempts to smooth the tetrahedral mesh. Therefore, the cell-centered approach described in §7 cannot accurately approximate the true solution on tetrahedral meshes. Experimentally we observe that the enhanced method gives $O(h^2)$ accuracy for the pressure and $O(h)$ accuracy for the flux; however, since there are now Lagrange multiplier pressures on every face, this is not necessarily an improvement of the hybrid form of the standard mixed method.

11. An observation on the standard mixed method. Recall from the last section that when K is discontinuous and $\tilde{V}_h = V_h$ has continuous normal components, we are unable to properly approximate $\tilde{\mathbf{u}}$, since it is then discontinuous. Numerically, it has been observed that the standard mixed method performs well even when K is discontinuous. Evidently, in this case $\tilde{\mathbf{u}}$ is automatically approximated in some discontinuous space. This is indeed true, as we now show.

We rewrite the standard method (3.1.2) in the following form. Find $\mathbf{U} \in V_h$, $\tilde{\mathbf{U}} \in \tilde{V}_h$, $P \in W_h$, and $\lambda \in \Lambda_h^N$ satisfying (3.1.2b)–(3.1.2c) and

$$(11.1a) \qquad (\tilde{\mathbf{U}}, \mathbf{v}) - (P, \nabla \cdot \mathbf{v})$$
$$= -\langle g^D, \mathbf{v} \cdot \nu \rangle_{\Gamma^D} - \langle \lambda, \mathbf{v} \cdot \nu \rangle_{\Gamma^N}, \quad \mathbf{v} \in V_h,$$
$$(11.1b) \qquad (K^{-1}\mathbf{U}, \tilde{\mathbf{v}}) = (\tilde{\mathbf{U}}, \tilde{\mathbf{v}}) \qquad\qquad \tilde{\mathbf{v}} \in \tilde{V}_h.$$

Since $V_h \subset \tilde{V}_h$, these two equations combine to form (3.1.2a).

Suppose that $\tilde{V}_h = \bar{V}_h$ is fully discontinuous, and take the orthogonal decom-

position $\tilde{V}_h = V_h \oplus V_h^d$ with respect to the L^2 inner product, and expand

$$(11.2) \qquad \tilde{\mathbf{U}} = \tilde{\mathbf{U}}^c + \tilde{\mathbf{U}}^d, \quad \tilde{\mathbf{U}}^c \in V_h \text{ and } \tilde{\mathbf{U}}^d \in V_h^d.$$

Then $\tilde{\mathbf{U}}$ can be replaced by $\tilde{\mathbf{U}}^c$ in (11.1a) by orthogonality. Moreover, (11.1b) becomes the pair of equations

$$(11.3a) \qquad (K^{-1}\mathbf{U}, \tilde{\mathbf{v}}^c) = (\tilde{\mathbf{U}}^c, \tilde{\mathbf{v}}^c) \quad \tilde{\mathbf{v}}^c \in V_h,$$

$$(11.3b) \qquad (K^{-1}\mathbf{U}, \tilde{\mathbf{v}}^d) = (\tilde{\mathbf{U}}^d, \tilde{\mathbf{v}}^d) \quad \tilde{\mathbf{v}}^d \in V_h^d.$$

That is, the combination of (11.1a) and (11.3a), together with (11.1c), (3.1.2b)–(3.1.2c) forms the usual mixed method, solvable without reference to $\tilde{\mathbf{U}}$. Then (11.3a) gives the continuous part of $\tilde{\mathbf{U}}$, and (11.3b) gives the discontinuous part.

12. Some conclusions. The cell-centered finite difference method has been defined rigorously as a quadrature approximation of the expanded mixed method for general meshes of quadrilaterals, triangles, hexahedra, and tetrahedra. We saw both theoretically and computationally that the method is accurate and efficient on smooth meshes that are either logically rectangular or triangular with six triangles per interior vertex (it appears to be about twice as fast as competing methods). On hierarchical meshes, the method loses accuracy, but the enhanced variant of the method does not. This enhanced method is more efficient than the hybrid form of the mixed method in hierarchical settings where the coarse elements are sufficiently refined so that the enhanced method uses many fewer Lagrange multiplier unknowns than the hybrid method. Meshes of tetrahedral elements, however, are never smooth, so the cell-centered finite difference method always loses accuracy and the hybrid method or the enhanced method with Lagrange multipliers on every face should be used.

REFERENCES

[1] D. A. ANDERSON AND H. N. SHARPE, *Orthogonal curvilinear grid generation with preset internal boundaries for reservoir simulation*, SPE 21235, in Proceedings, Eleventh SPE Symposium on Reservoir Simulation, Anaheim, California, Society of Petroleum Engineers, Feb. 17-20, 1991, pp. 323-339.

[2] T. ARBOGAST, M. F. WHEELER, AND I. YOTOV, *Mixed finite elements for elliptic problems with tensor coefficients as cell-centered finite differences*, to appear.

[3] D. N. ARNOLD AND F. BREZZI, *Mixed and nonconforming finite element methods: implementation, postprocessing and error estimates*, Modélisation Mathématiques et Analyse Numérique, 19 (1985), pp. 7–32.

[4] I. BABUŠKA, *The finite element method with Lagrangian multipliers*, Numer. Math., 20 (1973), pp. 179–192.

[5] F. BREZZI, *On the existence, uniqueness, and approximation of saddle point problems arising from Lagrangian multipliers*, RAIRO Anal. Numér., 2 (1974), pp. 129–151.

[6] F. BREZZI, J. DOUGLAS, JR., R. DURÀN, AND M. FORTIN, *Mixed finite elements for second order elliptic problems in three variables*, Numer. Math., 51 (1987), pp. 237-250.

[7] F. BREZZI, J. DOUGLAS, JR., M. FORTIN, AND L. D. MARINI, *Efficient rectangular mixed finite elements in two and three space variables*, RAIRO Modèl. Math. Anal. Numèr.,

21 (1987), pp. 581-604.

[8] F. Brezzi, J. Douglas, Jr., and L. D. Marini, *Two families of mixed elements for second order elliptic problems*, Numer. Math., 88 (1985), pp. 217-235.

[9] F. Brezzi and M. Fortin, *Mixed and hybrid finite element methods*, Springer-Verlag, New York, 1991.

[10] Zhangxin Chen, *BDM mixed methods for a nonlinear elliptic problem*, J. Comp. Appl. Math., 53 (1994), pp. 207–223.

[11] Zhangxin Chen and J. Douglas, Jr., *Prismatic mixed finite elements for second order elliptic problems*, Calcolo, 26 (1989), pp. 135-148.

[12] P. G. Ciarlet, *The finite element method for elliptic problems*, North-Holland, New York, 1978.

[13] L. C. Cowsar, J. Mandel, and M. F. Wheeler, *Balancing domain decomposition for cell-centered finite differences*, Math. Comp., to appear.

[14] L. C. Cowsar, A. Weiser, and M. F. Wheeler, *Parallel multigrid and domain decomposition algorithms for elliptic equations*, in Fifth International Symposium on Domain Decomposition Methods for Partial Differential Equations, D. Keyes et al., eds., SIAM, Philadelphia, 1992, pp. 376–385.

[15] P. J. Davis, *Interpolation and Approximation*, Dover Publications, New York, 1975.

[16] J. Douglas, Jr. and J. E. Roberts, *Global estimates for mixed methods for second order elliptic equations*, Math. Comp., 44 (1985), pp. 39-52.

[17] T. F. Dupont, and P. T. Keenan, *Superconvergence and postprocessing of fluxes from lowest order mixed methods on triangles and tetrahedra*, Technical Report TR95–03, Department of Computational and Applied Mathematics, Rice University (1995), to appear.

[18] R. Durán, *Superconvergence for rectangular mixed finite elements*, Numer. Math., 58 (1990), pp. 287–298.

[19] R. E. Ewing, R. D. Lazarov, and Junping Wang, *Superconvergence of the velocity along the Gauss lines in mixed finite element methods*, SIAM J. Numer. Anal., 28 (1991), pp. 1015–1029.

[20] L. Gastaldi and R. Nochetto, *Optimal L^∞-error estimates for nonconforming and mixed finite element methods of lowest order*, Numer. Math., 50 (1987), pp. 587-611.

[21] R. Glowinski, W. Kinton, and M. F. Wheeler, *Acceleration of domain decomposition algorithms for mixed finite elements by multi-level methods*, in Third International Symposium on Domain Decomposition Methods for Partial Differential Equations, T. F. Chan et al., eds., SIAM, Philadelphia, 1990, pp. 263-289.

[22] R. Glowinski and M. F. Wheeler, *Domain decomposition and mixed finite element methods for elliptic problems*, in First International Symposium on Domain Decomposition Methods for Partial Differential Equations, R. Glowinski et al., eds., SIAM, Philadelphia, 1988, pp. 144-172.

[23] P. T. Keenan, *RUF 1.0 user manual: the Rice unstructured flow code*, Technical Report TR94–30, Department of Computational and Applied Mathematics, Rice University (1994).

[24] P. T. Keenan, *An efficient postprocessor for velocities from mixed methods on triangular elements*, Technical Report TR94–22, Department of Computational and Applied Mathematics, Rice University (1994).

[25] J. Koebbe, *A computationally efficient modification of mixed finite element methods for flow problems with full transmissivity tensors*, Numer. Meth. for PDE's, 9 (1993), pp. 339–355.

[26] H.-O. Kreiss, T. A. Manteuffel, B. K. Swartz, B. Wendroff, and A. B. White, *Supra-convergent schemes on irregular grids*, Math. Comp., 47 (1986), pp. 511–535.

[27] M. Nakata, A. Weiser, and M. F. Wheeler, *Some superconvergence results for mixed finite element methods for elliptic problems on rectangular domains*, in The Mathematics of Finite Elements and Applications V, J. R. Whiteman, ed., Academic Press, London, 1985.

[28] J. C. NEDELEC, *Mixed finite elements in* $\mathbf{R}^3$, Numer. Math., 35 (1980), pp. 315-341.

[29] V. J. PARR, *Preconditioner schemes for elliptic saddle-point matrices based upon Jacobi multi-band polynomial matrices*, Ph.D. Thesis, Dept. of Computational and Applied Math., Rice University, 1994.

[30] D. W. PEACEMAN, *Fundamentals of numerical reservoir simulation*, Elsevier, Amsterdam, 1977.

[31] R. A. RAVIART AND J. M. THOMAS, *A mixed finite element method for 2nd order elliptic problems*, in Mathematical Aspects of the Finite Element Method, Lecture Notes in Math, 606, Springer-Verlag, New York, 1977, pp. 292-315.

[32] T. F. RUSSELL AND M. F. WHEELER, *Finite element and finite difference methods for continuous flows in porous media*, Chapter II, in The Mathematics of Reservoir Simulation, R. E. Ewing, ed., Frontiers in Applied Mathematics 1, Society for Industrial and Applied Mathematics, Philadelphia, 1983, pp. 35–106.

[33] T. RUSTEN, *Iterative methods for mixed finite element systems*, Ph.D. Thesis, Dept. of Informatics, University of Oslo, 1991.

[34] J. M. THOMAS, These de Doctorat d'etat, à l'Universite Pierre et Marie Curie, 1977.

[35] A. N. TIKHONOV AND A. A. SAMARSKII, *Homogeneous differenc schemes on non-uniform nets*, Zh. Vychisl. Mat. i Mat. Fiz., 2 (1962), pp. 812–832, in Russian; U.S.S.R. Comput. Math. and Math. Phys., 2 (1962), pp. 927–953, in English.

[36] A. WEISER AND M. F. WHEELER, *On convergence of block-centered finite-differences for elliptic problems*, SIAM J. Numer. Anal., 25 (1988), pp. 351-375.

[37] M. F. WHEELER, K. R. ROBERSON, AND A. CHILAKAPATI, *Three-dimensional bioremediation modeling in heterogeneous porous media*, in Computational Methods in Water Resources IX, Vol. 2: Mathematical Modeling in Water Resources, T. F. Russell *et al.*, eds., Computational Mechanics Publications, Southampton, U. K., 1992, pp. 299–315.